

*Acherontiscus caledoniae*, the earliest heterodont and durophagous tetrapod

Jennifer A. Clack<sup>1</sup>, Marcello Ruta<sup>2</sup>, Andrew R. Milner<sup>3</sup>, John E. A. Marshall<sup>4</sup>, Timothy R. Smithson<sup>1</sup> and Keturah Z. Smithson<sup>1</sup>.

<sup>1</sup> University Museum of Zoology, Downing St., Cambridge, Dowing St., Cambridge CB2 3EJ, UK

<sup>2</sup> School of Life Sciences, University of Lincoln, Joseph Banks Laboratories, Green Lane, Lincoln LN6 7DL, UK

<sup>3</sup> Department of Earth Science, Natural History Museum, Cromwell Road, London SW7 5BD, UK

<sup>4</sup> School of Ocean & Earth Science, National Oceanography Centre, University of Southampton, Waterfront Campus, European Way, Southampton SO14 3ZH, UK  
JAC <https://orcid.org/0000-0003-0017-5831>

MR <https://orcid.org/0000-0002-6151-0704>

TRS <https://orcid.org/0000-0002-6546-1145>

The enigmatic tetrapod *Acherontiscus caledoniae* from the Pendleian stage of the Early Carboniferous shows heterodontous and durophagous teeth, representing the earliest known examples of significant adaptations in tetrapod dental morphology.

Tetrapods of the Late Devonian and Early Carboniferous (Mississippian), now known in some depth, are generally conservative in their dentition and body morphologies. Their teeth are simple and uniform, being cone-like and sometimes recurved at the tip.

Modifications such as keels occur for the first time in Early Carboniferous Tournaisian tetrapods. *Acherontiscus*, dated as from the Pendleian stage, is notable for being very

small with skull length of about 15 mm, having an elongate vertebral column, and being limbless. Cladistic analysis places it close to the Early Carboniferous adelospondyls, aïstopods, and colosteids, and supports the hypothesis of ‘lepospondyl’ polyphyly.

Heterodonty is associated with a varied diet in tetrapods, while durophagy suggests a diet that includes hard tissue such as chitin or shells. The mid-Carboniferous saw a significant increase in morphological innovation among tetrapods, with an expanded diversity of body forms, skull shapes, and dentitions appearing for the first time.

Key Words: Early Carboniferous, earliest Serpukhovian (‘Namurian’), adelospondyls, aïstopods, colosteids, ‘lepospondyl’ polyphyly

## 1. Introduction

The Early Carboniferous Period (Mississippian) saw the dawn of continental tetrapod diversity. Pentadactylous limbs [1], increased eye size [2], steep-sided skulls [3], and a wide range of body sizes are found among Tournaisian forms [4]. However, body shape and dental morphologies appear to have remained essentially conservative. By the later Viséan stage, tetrapods had begun to assume more varied body morphologies. Some groups had reduced or lost their limbs and developed elongate vertebral columns [5-7].

The foundations of the tetrapod crown group had been laid [8]. Little attention has so far been paid to dental morphologies, overlooked as conservative. One of the few modifications noted among Tournaisian tetrapods was the appearance of lateral keels on the tooth crowns of a large un-named tetrapod [4]. Here we report the earliest documented example, from the Pendleian (earliest Serpukhovian stage, late Mississippian), of both heterodont and durophagous dental adaptations in the small, limbless and elongate tetrapod, *Acherontiscus caledoniae*. Furthermore, we note the contemporary

evolution of three clades of limbless, elongate tetrapods, each with its own specialized dentition (5-7).

*Acherontiscus* was first described by Carroll [9], who recognized its significance, and illustrated but did not discuss its heterodont dentition. More recently its heterodonty was further revealed by micro-CT scanning [10]. Carroll [9] considered *Acherontiscus* to be a 'lepospondyl', an assemblage of small tetrapods with solid 'holospondylous' vertebral centra and lacking a spiracular or 'otic' notch at the back of the skull. Now recognized as probably a polyphyletic array [e.g. 7], 'lepospondyls' are split among various Palaeozoic tetrapod groups, leaving the relationships of *Acherontiscus* unresolved. Other small, elongate and limbless tetrapods from the Pendleian include aïstopods and adelospondyls: the relationships of the latter two to *Acherontiscus* have remained little explored.

## 2. Material and Methods

(a) Holotype and only specimen: National Museums Scotland (NMS) G 1967.13.1. Purchased by the museum in the late 19<sup>th</sup> century, the specimen of *Acherontiscus caledoniae* consists of a skull about 15 mm long (figure 1) and an elongate, diplospondylous vertebral column, the latter in natural mould. There are no field or locality data, but recent work has refined the dating to the Pendleian (early Serpukhovian) stage (electronic supplementary material S1). Although the locality remains uncertain, the specimen is regarded as most likely originating from one of the 'Ironstone' horizons from a colliery in the region of Loanhead, Scotland, probably Burghlee [11]; see also Andrews and Brand [in ref 5].

(b) Visualization. Micro-CT at NHM Zeiss versa: Source: 110kV, 10W; Camera Binning 1; Exposure: 2 Seconds; Rotation: 180 (Fan); Projections 2501; Source

76 Distance -50.01mm; Detector Distance: 65.95mm; Filter HE1 (Silicon Dioxide); Lens  
 77 Objective 0.4X; resolution 14.873  $\mu\text{m}$ ; slice dimensions, X 2008, Y 2048, Z2034.  
 78 Segmentation using Materialise's Interactive Medical Image Control System (MIMICS)  
 79 Research v18.  
 80 Microphotography. For figure 1a, Nikon D60 fitted with a AF-S DX Micro-Nikkor  
 81 40mm f/2.8G Macro lens. For figure 1c, Z-stacks were taken on a Leica S8APO  
 82 dissecting microscope (Leica Microsystems (UK) Ltd, with a Nikon D5200 camera and  
 83 Nikon Camera Control Pro 2 using a MacBook Pro computer and rendered into a single  
 84 focused image with Helicon Focus.  
 85 See electronic supplementary material S2 for the micro-CT scan data and three  
 86 movies: *Acherontiscus* left lower jaw removed (6.6MB); *Acherontiscus* left lower jaw  
 87 (2.5 MB); and *Acherontiscus* skull roof (4.2MB).  
 88 (c) Palynological analysis  
 89 Two samples (Ach-1 (0.1 g) and Ach-2 (<0.1 g) of the matrix of *Acherontiscus* were  
 90 surface inspected for contamination or consolidant from curation and conservation.  
 91 Both appeared clean fragments and represented single laminae from the sample. These  
 92 very small samples were processed using screw topped Savillex™ PFA digestion  
 93 vessels and small sieves to preserve the residue and prevent any contamination. Treated  
 94 uncrushed with 60% HF for 16 hours, they failed to disaggregate because of the highly  
 95 organic matrix. They were then decant-washed clean of HF and subjected to 15 hours in  
 96 fuming nitric acid. Ach-2 disaggregated readily but Ach-1 failed to dissolve so was  
 97 crushed down to sub-mm size and returned to fuming nitric acid for a further 15 hours,  
 98 which was successful. The residues were diluted in water and sieved at 15  $\mu\text{m}$  to  
 99 concentrate the spores. Both samples contained residual minerals including mica and  
 100 were returned to the digestion vessels for 12 hours in 60% HF and resieved at 15  $\mu\text{m}$



before storage. Multiple slides of the very small amount of residue was mounted using Elvacite 2044™ to produce one sparse, poorly preserved but workable palynological assemblage from Ach-1 and a better assemblage from Ach-2 (electronic supplementary material S1, figures S1,2 and table S1).

#### (d) Phylogenetic analysis

To evaluate the phylogenetic position of *Acherontiscus*, we assembled a new data matrix consisting of 260 characters and 57 taxa, representing a modified and expanded version of the matrix in Clack *et al.* [4]. All 213 characters in that matrix were re-assessed and their scores re-checked for each taxon, and 47 characters were added (electronic supplementary data S3; new characters marked with asterisks). In order to cover a wider cross section of early tetrapod diversity, in addition to *Acherontiscus*, we added 11 taxa to the Clack *et al.* [4] matrix. Both maximum parsimony using different character weighting schemes, and Bayesian inference analyses were performed. Before parsimony analyses were carried out, the matrix was scrutinised for possible occurrences of “rogue” taxa [12] that could be safely removed, using the *Claddis* library [13] in the R environment for statistical computing and graphics (<https://cran.r-project.org>) (electronic supplementary material S3 and figure S3).

### 3. Results

#### (a) Specimen Description

The skull has been crushed laterally obscuring the left side of the head and lower jaw, and remains hard to interpret despite high-resolution micro-CT scanning (see electronic supplementary material S2 stored on Dryad for movies). Some of the skull bones in *Acherontiscus* are tightly knit obscuring the sutures, suggesting that the animal was not a juvenile, although other bones are displaced. As preserved, the skull has a short snout

with a relatively large, laterally placed orbit, and a long postorbital region, but skull height and interorbital distance remain hard to estimate. The rear margin of the skull table is convexly curved, and may consist of either one single or two large postparietals (figures 1, 2), with a small tabular at each corner. The lacrimals and nasals are short, but the frontals are elongate and tapered anteriorly to be deeply wedged between the nasals. Other parts of the cheek and skull roof are difficult to separate. Lacrimals, nasals, premaxillae and maxillae bear lateral line pores, some of which are elongate (figure 2). Parts of the palate and braincase are preserved, showing the pterygoids with large but sparsely distributed denticles. The palatines bear small teeth, the ectopterygoid larger ones, and the vomers do not appear to be preserved (figure 2). The parasphenoid is narrowly triangular, and the sphenethmoid is a broad V in cross-section, appearing firmly attached to the skull roof, and bearing a double row of crests for attachment of the parasphenoid (figure 2). The dentary houses at least 18 teeth although the tip of the jaw is missing, the maxilla bears about 21, and the premaxilla 11 or 12. The pattern of divergent number of upper versus lower teeth is not uncommon in early tetrapods, and of particular interest for our phylogenetic results, occur in the colosteids [14] and the Tournaisian *Aytonerpeton* [4]. Substantial branchial bars are preserved, which are essentially similar to those of the contemporary adelogyrinids [5,10].

Micro-CT scans reveal the dentary tooth row to be dominated by four enlarged teeth at its centre, with smaller teeth anteriorly and posteriorly (figures 1, 2). On the right side of the jaw, the bases of the large maxillary teeth and some of their tooth crowns have been broken through: none shows any sign of labyrinthodont infolding in the enamel. The tips of two of the enlarged teeth have penetrated the skull roof as the dentary was folded over by crushing, and are laterally compressed with apicobasally ridged crowns and crenellated tips (figure 1). The maxilla has a similar number of

enlarged teeth as the dentary (tips are not preserved) and although they are less enlarged than those on the dentary, they would have occluded with them (figures 1, 2).

The lower jaw bears lateral line pores and has a surangular lateral line canal as well as a submandibular canal (figure 2). The probable third and second coronoids bear similar-sized denticles to the pterygoids (figure 2). The lower jaw also has a high surangular crest which would have supported the jaw-closing musculature and allowed a more powerful bite at the level of the enlarged dentition. A single Meckelian fenestra is present (figure 2). We can confirm the diplospondylous nature of the vertebral column as described by Carroll [9], but do not describe the postcranial skeleton further.

#### (b) Phylogenetic analysis

No taxa were identified as being suitable for safe taxonomic deletion. The unweighted parsimony analysis yielded 312 filtered trees at 1237 steps, with ensemble consistency index (C. I.) of 0.2753 (excluding uninformative characters) and ensemble retention index (R. I.) of 0.5699. Bootstrap and jackknife support were generally low for most nodes. Reweighting characters by the maximum value of their rescaled consistency index resulted in one tree (199.18768 steps; C. I. = 0.4542; R. I. = 0.7363). A single tree was retrieved after each implied weighting analysis, for any given value of the  $K$  constant of concavity.

Regardless of optimality criteria and search settings, *Acherontiscus* is consistently retrieved as sister taxon to the recently described Tournaisian tetrapod *Aytonerpeton* [4], and the (*Acherontiscus* + *Aytonerpeton*) clade forms the sister group to adelospondyls (*Adelogyrinus*, *Adelospondylus*, *Dolichopareias* [16]) (figure. 3). However, nodal support for these groupings is invariably poor (electronic supplementary material S1 and figure S3).

Under parsimony, the ((*Acherontiscus* + *Aytonerpeton*) + adelospondyls) clade emerges as sister group to a clade consisting of aïstopods (*Lethiscus* [7]; *Oestocephalus* [15]; and nectrideans (*Sauropleuria*; *Ptyonius*; *Urocordylus* [16]). These appear in all analyses as sister group to a tetrapod array including, inter alia, colosteids and the Devonian *Tulerpeton* [17]. The implied weighting analysis resulted in few though significant changes in the position of some taxa, chiefly stem-tetrapods. Among these, *Tulerpeton* appears in a more conventional position as the most derived Devonian stem-tetrapod, and a clade consisting of *Ossirarus*[4] and *Ossinodus* [18] branches between *Ventastega* [19] (anti-crownward) and *Ymeria* [20] (crownward) (figure 3).

In the Bayesian analysis, few clades emerge with moderate to strong support (Bayesian credibility values) and most taxa and groups are collapsed. Among the clades supported by the Bayesian analysis are (aïstopods + nectrideans) and ((*Acherontiscus* + *Aytonerpeton*) + adelospondyls) (figure 3).

#### **4. Discussion**

##### **(a) Heterodonty in non-mammalian tetrapods**

The occurrence of heterodonty and durophagy in such an early tetrapod, and in particular the form of the exposed tips of the enlarged dentary teeth is unprecedented. That these tips represent places where the infolded enamel has been removed by erosion to reveal the underlying dentine can be ruled out. Labyrinthodont infolding is usually (although not exclusively) associated with large teeth. Unfortunately, the resolution of the scan does not permit us to determine whether it was present in any of the smaller teeth, nor to see cross sections of the larger teeth. Furthermore, the dentary teeth are compressed laterally, whereas the skull is compressed dorsoventrally. The resolution of the scan is insufficient to show whether the tips of the smaller teeth are similarly

shaped, or how thick the enamel may have been relative to the dentine. Enamel thickness significantly affects a tooth's function [21].

Among Palaeozoic fossil forms, a few Late Carboniferous and several Early Permian microsaurs show a degree of heterodonty (e.g. *Pantylus* [16]), but the most similar tooth distribution and morphology is seen in the Early Permian captorhinid eureptile *Opisthodontosaurus* from North America [22]. Formerly considered the earliest example of this kind of heterodonty, *Opisthodontosaurus* is more than 50 Myr younger than *Acherontiscus*. Furthermore, the skull of *Opisthodontosaurus* is about 2.5 times the size of that of *Acherontiscus*, and unlike the limbless *Acherontiscus* with its lateral lines, the captorhinid *Opisthodontosaurus* would have been terrestrial. The convergence in dentition, including the ribbed tips of the enlarged teeth, is therefore surprising. It may indicate an early example of convergence towards an effective crushing and slicing action powered by a strong bite force.

Heterodonty is closely tied to diet and occurs associated with omnivory, insectivory and herbivory [23]. A diet of arthropods with tough chitin was proposed for *Opisthodontosaurus* [22]. *Acherontiscus* might have fed on aquatic molluscs or crustaceans, including ostracods with their hard carapaces and which are abundant in the matrix from the fossil. The robust, high surangular crest associated with the derived dentition may indicate a new level of biomechanical complexity in the jaws of early tetrapods, and might imply the presence of highly differentiated jaw adductor muscles, with a powerful bite.

The arthropod fauna of the mid-Carboniferous is poorly known, but as an aquatic tetrapod, and in view of its small size, *Acherontiscus* is unlikely to have had access to fully terrestrial forms such as myriapods, although it may have had access to smaller aquatic crustaceans.

225           Apicobasal ridges are not uncommon among tetrapods, for example the Late  
226 Triassic rhynchocephalian *Eilenodon*, as well as various other extinct taxa [24]. In  
227 *Eilenodon*, it is thought to be associated mainly with herbivory, and especially  
228 consumption of lycopsid stems, enhancing tooth penetration with additional abrasive  
229 edges and greater grip. Patterns of heterodonty can appear similar in animals with  
230 similar diets, even across unrelated species [25, 26]. Palynology implies that the  
231 environment from which *Acherontiscus* was recovered was a small body of still water  
232 surrounded by small herbaceous lycopsids. Larger *Lepidodendron* lycopsids formed a  
233 forest further away at other times (electronic supplementary material S1). However,  
234 although lycopsids were very common in the likely habitat of *Acherontiscus*, there is no  
235 direct evidence that these formed one of its food sources. The first tetrapod herbivores  
236 are not thought to have evolved before the latest Carboniferous [27].

237           Heterodonty together with a durophagous morphology also occurs widely, but  
238 sporadically, among both later Palaeozoic and Mesozoic lineages. It appears in stem  
239 amniotes such as diadectids [28], and in crown amniotes such as the captorhinid  
240 *Opisthodontosaurus* [22], notosuchian crocodyliforms [29], various lineages of  
241 herbivorous dinosaurs [30], the sauropterygian placodonts [31], and Mesozoic and  
242 modern lepidosauromorphs [24,32,33]. In amphibians and their stem group, it is very  
243 rare: some early tetrapods including temnospondyls show size heterodonty and some  
244 fossil dissorophoid temnospondyls show bicuspid teeth, but none shows durophagy  
245 [34]; some modern caecilians have multicusped teeth [35]; and heterodonty is absent  
246 from anurans and urodeles.

247           Fishes (chondrichthyans, actinopterygian fishes especially teleosts) and  
248 mammals are the groups that have been most studied for the developmental genetics of  
249 heterodonty [e.g.36, 37], although there has been recent work on lizards (38,39).

However, dentitions, including heterodonty, appear to be engendered by transcription factors in the jaw that are conserved across all vertebrates [25,40]. Once gained, heterodonty is also apparently easily lost and can also be regained because the pattern of the genetic code is still present [40]. Heterodonty is essentially the norm in synapsids and throughout mammals, and occurs apparently independently among many families of modern lizards [42]. Mammals differ from other tetrapods in their enamel construction, but in both cases, it is the differential deposition of hard tissue that is used to create details of their external form [26,41].

Heterodonty in early tetrapods could have been associated with the diversification of body form which they underwent in the mid-Carboniferous, exploiting new and varied food sources for which differently patterned teeth would have been required. The relationship between heterodonty and diet could have been driven by a process of correlated progression [43] between diet and dentitions as tetrapods explored different terrestrial and aquatic niches emerging during the Early and mid-Carboniferous, so the expectation might be that more should eventually be found in the fossil record.

#### (b) Other palaeobiological inferences

Our results suggest that the evolution of limbless tetrapods with elongate postcrania occurred three times in the late Viséan and early Serpukovian: in aïstopods [16], in adelospondyls [16], and in *Acherontiscus*. Each has a different and specialized form of dentition, although what each was exploiting is unknown. Although these three are placed close together in our analyses, it appears that they developed their dental conditions and limblessness independently from a common limbed ancestor, whose descendants may also include nectrideans and/or colosteids. These groups also show some members with a tendency for trunk or tail elongation. The Bayesian analysis

breaks apart former stem amniote taxa which are placed variously along the spine, with microsaur as an independent group. All analyses place colosteids, nectrideans plus aïstopods and a clade containing *Acherontiscus*, *Aytonerpeton* and the adelospondyls all as stem tetrapods, remote from stem amphibians, stem amniotes and microsaur, further supporting the hypothesis of the polyphyly of ‘lepospondyls’.

One fauna contemporary with that of *Acherontiscus*, from the Burghlee Ironstone in the region of Loanhead, includes several taxa with specialised dentitions. It includes actinopterygians such as *Eurynotus* [44] and *Drydenius* [45] with durophagous adaptations, probably the enigmatic tetrapod *Caerorhachis* [46] with a totally denticulated lingual lower jaw surface and palate, a new small lungfish with an unusual durophagous dentition [47], and a range of taxa with numerous homodont chisel-shaped teeth (adelospondyls [5], *Doragnathus* [48]), and the broad, shallow-headed baphetid *Spathicephalus* [49]. All the tetrapod taxa except *Spathicephalus* appear unique to this area of Scotland, indicating an unusual set of conditions for the mid-Carboniferous.

In the mid-Carboniferous, the Loanhead area of Scotland was in the equatorial region of the Earth [50]. Today, equatorial rain forest is home to the greatest diversity of life on Earth. The same is likely to have been true in the Carboniferous, providing the impetus for further diversification of tetrapods.

## 5. Conclusions

The enigmatic *Acherontiscus* plus the fauna from Loanhead, exemplify and illustrate the expanded range of skull and body morphologies and dental organisation among tetrapods that began to emerge in the mid-Carboniferous. This interval was key to the great diversification of tetrapods, which culminated in the evolution of amniotes in the early Late Carboniferous. Following the Hangenberg Event at the end of the Devonian,



large plants initially disappeared, recovering slowly through the Tournaisian [4,51]. As dense floras and more complex ecosystems emerged throughout the Viséan, new niches became available in continental ecosystems, particularly in equatorial regions, and were exploited by tetrapods.

Consistent with new finds from the Tournaisian of tetrapods [1,4] and lungfishes [52], many vertebrate clades appear to have arisen much earlier than previously considered. Much must still be missing from the fossil record of the Early Carboniferous, and we might expect to find further examples of more specialised adaptations among tetrapods of that time. Continental deposits of the Early Carboniferous deserve further exploration and study.

#### **Data Availability**

Micro-CT scan data and three movies available on Dryad on <https://datadryad.org/review?doi=doi:10.5061/dryad.0pc151n>

#### **Competing interests**

The authors declare there are no competing interests.

#### **Funding**

NERC consortium Grant (NE/J022713/1 Cambridge JAC, TRS, KZS: NE/J021091/1 Southampton, JEAM); Leverhulme Trust Emeritus Fellowship to JAC. ARM received no funding.

#### **Author contributions**

ARM and MR initiated the study, MR carried out phylogenetic analyses, JAC and KZS contributed new micro-CT data, segmentation and skull reconstructions, JEAM contributed palynological dating and environmental analysis. JAC, MR, ARM, TRS KZS and JEAM contributed to writing the paper.

326

## 327 **Acknowledgements**

328 Acknowledgements: Stig Walsh, for curation and loan of specimens, Andrew Ross, for  
329 advice on Viséan arthropods (National Museums Scotland: NE/J020621/1); Malcolm  
330 Burrows and José Casal-Jimenez (Cambridge Zoology) and Javier Ortega-Hernández  
331 and Julie Sarmiento Ponce (Cambridge Earth Sciences) for microphotography; Farah  
332 Ahmed, Amin Garbout and Brett Clark (Natural History Museum, London [NHM]) for  
333 Zeiss Versa scanning; Marc Jones (NHM), Abigail Tucker (Kings College London), and  
334 Jason Head (University Museum of Zoology, Cambridge) for discussion of heterodonty  
335 in tetrapods.

336

## 337 **References**

- 338 1. Smithson TR, Wood SP, Marshall JEA and Clack JA. 2012 Earliest Carboniferous  
339 tetrapod and arthropod faunas from Scotland populate Romer's Gap. *Proc. Natl*  
340 *Acad. Sci.* **109**, 4532-4537.
- 341 2. MacIver MA, Schimtz, L, Mugan, U, Murphey T, Mobley CD. 2017 Massive  
342 increase in visual range preceded the origin of terrestrial vertebrates. *Proc. Natl*  
343 *Acad. Sci.* E2375-2384
- 344 3. Clack JA, Finney SM. 2005 (for 2004) *Pederpes finneyae*, an articulated tetrapod  
345 from the Tournaisian of western Scotland. *J. Syst. Palaeo.* **2**, 311-346.
- 346 4. Clack JA, Bennett CE, Carpenter DK, Davies S J, Fraser NC, Kearsey TI,  
347 Marshall JEA, Millward D, Otoo BKA, Reeves EJ, Ross AJ, Ruta M, Smithson  
348 KZ, Smithson TR, Walsh S. 2017 Phylogenetic and Environmental Context of a  
349 Tournaisian Tetrapod Fauna. *Nature Ecol. and Evol.* **1**, 0002 doi:10.1038/s41559-  
350 016-0002

- 351 5. Andrews SM, Carroll RL. 1991 The order Adelospondyli. *Trans R. Soc. Edinb.*  
352 (*Earth Sci.*) **82**, 239-275.
- 353 6. Wellstead CF, 1982 A Lower Carboniferous aistopod of Scotland. *Palaeontology*  
354 **25**, 193-208.
- 355 7. Pardo JD, Szostakiwskyj M, Ahlberg PE, Anderson JS. 2017 Hidden  
356 morphological diversity among early tetrapods. *Nature* **546**, 642-645
- 357 8. Clack JA. 2012 *Gaining Ground: The origin and evolution of tetrapods*. (2<sup>nd</sup>  
358 Edn.) Bloomington Indiana, Indiana University Press.
- 359 9. Carroll RL, 1969 A new family of Carboniferous amphibians. *Palaeontology* **12**,  
360 537-548
- 361 10. Milner AR, Ruta M. 2013 *Acherontiscus caledoniae* – the first durophagous  
362 tetrapod and its phylogenetic implications. 61<sup>st</sup> *Symposium of Vertebrate*  
363 *Palaeontology and Comparative Anatomy Edinburgh. SVPCA.org Abstracts*  
364 *volume p. 58*
- 365 11. Smithson TR. 1985 Scottish Carboniferous amphibian localities. *Scot. J. Geol.* **21**,  
366 123-142.
- 367 12. Wilkinson M. 1996 Majority-rule reduced consensus trees and their use in  
368 bootstrapping. *Mol. Biol. Evol.* **13**, 437–444.
- 369 13. Lloyd GT. 2016 Estimating morphological diversity and tempo with discrete  
370 character-taxon matrices: implementation, challenges, progress, and future  
371 directions. *Biol. J. Linn. Soc.* **118**, 131-151.
- 372 14. Clack JA Milner AR. 2015 *Basal tetrapods. Handbook of Paleoherpetology*. Part  
373 3A1. (eds AR Milner, H-D Sues) Munich, Germany: Verlag Dr Friedrich Pfeil.

- 374 15. Anderson JS. 2003 Cranial anatomy of *Coloraderpeton brilli*, postcranial anatomy  
375 of *Oestocephalus amphiuminus*, and reconsideration of Ophiderpetontidae  
376 (Tetrapoda: Lepospondyl: Aïstopoda). *J. Vertebr. Paleont.* **23**, 532-543.
- 377 16. Carroll RL, Bossy, KA, Milner AC, Andrews SM, Wellstead CF. 1998  
378 *Lepospondyli: Handbook of Paleoherpetology*, Part 1. Munich, Germany: Verlag  
379 Dr Friedrich Pfeil.
- 380 17. Lebedev PA & Coates MI. 1995. The postcranial skeleton of the Devonian  
381 tetrapod *Tulerpeton curtum* Lebedev. *Zoo.J.Linn.Soc.* **114**, 307-348.
- 382 18. Warren AA. 2007 New data on *Ossinodus pueri*, a stem tetrapod from the Early  
383 Carboniferous of Australia. *J. Vert. Paleont.* **27**, 850-862.
- 384 19. Ahlberg PE, Clack JA, Luksevics E, Blom H, Zupins I. 2008 *Ventastega curonica*  
385 and the origin of tetrapod morphology. *Nature* **453**, 1199-1204
- 386 20. Clack JA, Ahlberg PE, Blom H, Finney SM. 2012 A new genus of Devonian  
387 tetrapod from East Greenland with new information on the lower jaw of  
388 *Ichthyostega*. *Palaeontology* **55**, 73-86
- 389 21. Freeman PW, Leman C. 2006 Punturing ability of idealized canine teeth: edged  
390 and non-edged shanks. *J. Zool.* **269**, 51-56 (doi:10.1111/j.1469-  
391 7998.2006.00049.x)
- 392 22. Reisz RR, LeBlanc ARH, Sidor CA, Scott D, May W. 2015 A new captorhinid  
393 from the Lower Permian of Oklahoma showing remarkable dental and mandibular  
394 convergence with microsaurian tetrapods. *Sci. Nat.* **102**, 50 doi: 1007/s00114-015-  
395 1299-y
- 396 23. Edmund AG, 1969 *Dentition. Biology of the Reptilia* (eds C Gans, A,d'A Bellairs,  
397 ST Parsons) New York, New York: Academic Press. 1, 117-200

24. Jones MEH, Lucas PW, Tucker AS, Watson AP, Sertich JJW, Foster JR, Williams R, Garbe U, Bevitt JJ, Salverni F. 2018 Neutron scanning reveals unexpected complexity in the enamel thickness of an herbivorous Jurassic reptile. *J. R. Soc Interface* **15**, 20180039. <http://dx.doi.org/10.1098/rsif.2018.0039>
25. Jernvall J, Thesleff I. 2012 Tooth shape formation and tooth renewal: evolving same signals. *Development* **139**, 3487-3497 doi:10.1242/dev.085084.
26. Stock DW. 2001 The genetic basis of modularity in the development and evolution of the vertebrate dentition. *Phil. Trans. R. Soc. Lond. B.* **356**, 1633-1653.
27. Sues H-P, Reisz RR. 1998 Origins and early evolution of herbivory in tetrapods. *Tr. Ecol. Evol.* **13**, 141-145.
28. Berman DS, Henrici AC, Kissel RA, Sumida SS, Martens T. 2004 A new diadectid (Diadectomorpha), *Orobates pabsti*, from the Early Permian of central Germany. *Bull. Carnegie Mus. Nat. Hist.* **35**, 1-36.
29. O'Connor PM, Sertich JJW, Stevens NJ, Roberts EM, Gottfried MD, Hieronymus TL, Jinnah ZA, Ridgely R, Ngasala SE, Temba J. 2010 The evolution of mammal-like crocodyliforms in the Cretaceous period of Gondwana. *Nature* **466**, 748-751.
30. Weishampel DB, Dodson P, Osmólska H. 2004 *The Dinosauria*. (2<sup>nd</sup> Edn.) Berkely CA: University of California Press.
31. Neenan JM, Li C, Rieppel O, Bernadini F, Tuniz C, Musico G, Scheyer T. 2014 Unique method of tooth replacement in durophagous placodont marine reptiles, with new data on the dentition of Chinese taxa. *J. Anat.* **224**, 603-613.
32. Meloro C, Jones MEH. 2012 Tooth and cranial disparity in the fossil relatives of *Sphenodon* (Rhynchocephalia) dispute the persistent 'living fossil' label. *J. Evol. Biol.* **25**, 2194-2209 <https://doi.org/10.1111/j.1420-9101.2012.02595.x>

33. Zahradnicek O, Buchtova M, Dosedelova H, Tucker, AS. 2014 The development of complex tooth shape in reptiles. *Front. Physiol.* **5**, article 74 doi: 10.3389/phys.2014.00074
34. Bolt JR. 1969 *Amphibamus grandiceps* as a juvenile dissorophid: evidence and implications. In *Mazon Creek Fossils* (ed. MH Nitecki), pp. 529-563 New York: Academic Press.
35. Kupfer A, Müller J, Antoniazzi MM, Jared C, Greven H, Nussbaum RS, Wilkinson, M. 2006 Parental investment by skin feeding in a caecilian amphibian. *Nature* **440**, 926-920
36. Ohazama A, Haworth KE, Ota MS, Khonsari RH, Sharpe PT. 2010 Ectoderm, endoderm, and the evolution of heterodont dentitions. *Genesis* **48**, 382-389.
37. Peterkova R., Hovorakova M, Peterka M, Lesot H. 201. Three-dimensional analysis of the early development of the dentition. *Austr. Dent. J.* **59**, (1 Suppl) 55-80. Doi: 10.1111/adj.12130
38. Ollonen J, Da Silva FO, Mahlow K, Di-Poi. 2011 Skull development, ossification pattern and adult shape in the emerging lizard model organism *Pogona vitticeps*: a comparison with other squamates. *Front. Physiol.* <https://doi.org/10.3389/fphys.2018.00278>
39. Handringan GR, Richman JM. 2011 Unicuspid and bicuspid crown formation in squamates. *J. Exp. Zool.* **316**, 598-608.
40. Peterkova R, Lesot H, Peterka M. 2006 Phylogenetic memory of developing mammalian dentition. *J. Exp. Zool.* **306**, 234-250.
41. Butler PM. 1956 The ontogeny of molar pattern. *Biol. Rev.* **31**, 30-70.
42. Smith K. 1993 The form of the feeding apparatus in terrestrial vertebrates: studies of adaption and constraint. In *The skull volume 3: functional and evolutionary*

- 448 *mechanisms* (eds J Hanken , BK Hall), pp.150-196. Chicago IL: Chicago  
 449 University Press.
- 450 43. Kemp TS. 2007 The concept of correlated progression as the basis of a mode for  
 451 the evolutionary origin of major new tax. *Proc. R. Soc B.* **274**, 1667-1673 doi:  
 452 10.1098/rspb.2007.0288.
- 453 44. Coates MI. 1994 Actinopterygian and acanthodian fishes from the Viséan of East  
 454 Kirkton, West Lothian, Scotland. *Trans. R. Soc. Edinb. (Earth Sci.)* **84**, 317-328.
- 455 45. Gardiner BG. 1967 Further notes on palaeoniscoid fishes with a classification of  
 456 the Chondrostei. *Bull. Brit. Mus. Nat. Hist.* **14**, 143-206.,
- 457 46. Ruta M, Milner AR Coates MI. 2002 The tetrapod *Caerorhachis bairdi* Holmes  
 458 and Carroll from the Lower Carboniferous of Scotland. *Trans. R. Soc. Edinb.*  
 459 *(Earth Sci.)* **92**, 229-261.
- 460 47. Smithson TR, Challands TJ, Smithson KZ. In press. Traquair's lungfish from  
 461 Loanhead: dipnoan diversity and tooth plate growth in the late Mississippian.  
 462 *Earth Envir. Sci Trans. R. Soc. Edinb.*
- 463 48. Smithson TR. 1980 A new labyrinthodont jaw from the Carboniferous of  
 464 Scotland. *Palaeontology* **23**, 915-923.
- 465 49. Smithson TR, Browne MAE, Davies SJ, Marshall JEA, Millward D, Walsh SA,  
 466 Clack JA. 2017 A new Mississippian tetrapod from Fife, Scotland, and its  
 467 environmental context. *Papers Palaeont.* **3**, 1-11.
- 468 50. *Deeptimemaps.com* 2018
- 469 51. Higgs K, Clayton G, Keegan JB. 1998 Stratigraphic and systematic palynology of  
 470 the Tournaisian rocks of Ireland. *Geol. Surv. Ireland, Spec. Pap.* **7**, 1-93.

52. Smithson TR, Richards KR, Clack JA. 2015 Lungfish diversity in Romer's Gap: reaction to the end-Devonian extinction. *Palaeontology* **59**, 29-44 doi: 10.1111/pala.12203

#### Figure legends

Fig. 1. *Acherontiscus caledoniae* holotype specimen NMS 1867.13.1. (a) Photograph of the skull and anterior postcranium. Scale bar 10 mm. (b) View of micro-CT image of the visible surface (approximately dorsal) of the skull. (c) Close-up of the crowns of two of the left dentary teeth showing apicobasal ridges. Scale bar 0.25 mm. (c) View of micro-CT image of the matrix-embedded (approximately ventral) surface of the skull. Abbreviations: crthy, ceratohyal; fro, frontal; hyob, hyobranchial; jug, jugal; L, left; lac, lacrimal; lr, lower; max, maxilla; ?par, ?parietal; popar, postparietal; porb, postorbital; premax, premaxilla; pteryg, pterygoid; R, right.

Fig. 2 *Acherontiscus caledoniae* Micro-CT images and skull and lower jaw reconstructions. (a) Left lower jaw ramus from micro-CT scan, mesial surface at left, lateral surface at right. (b) Left lower jaw ramus reconstructions mesial surface at left, lateral surface at right. (c) Skull reconstructions, palate at left, skull roof centre, lateral view at right. (d) Left premaxilla. (e) Right maxilla, part of the jugal and other circumorbital bones. (f) Camera lucida drawing of skull bones not visible in the scan. Scale bar 5 mm. (g) Micro-CT image of ventral surface of the skull with the lower jaw removed. (h) Micro-CT image of ventral surface of the skull with the lower jaw, marginal dentitigerous bones, and the parasphenoid removed. (i) Parasphenoid,



496 ventral view at left, dorsal view at right. Figures except (f) not to scale. Abbreviation:  
497 ?bocc, ?basioccipital; ectop, ectopterygoid, hyob, hyobranchial elements; jug, jugal,  
498 L, left, lac, lacrimal; max, maxilla; par, parietal; preart, prearticular; premax,  
499 premaxilla; psph, parasphenoid; pteryg, pterygoid; quj, quadratojugal; R, right; sphet,  
500 sphenethmoid.

501

502 Fig 3. Interrelationships of major group of early tetrapods. (a) strict consensus of  
503 312 equally parsimonious trees with unweighted characters. (b) single tree from  
504 parsimony analysis with characters reweighted by the maximum value of their  
505 rescaled consistency index. (c) strict consensus of ten trees, each obtained after  
506 applying implied weighting with a different integer value of the K constant of  
507 concavity (with K ranging from 1 to 10). d) Bayesian topology with credibility values  
508 appended to tree branches.

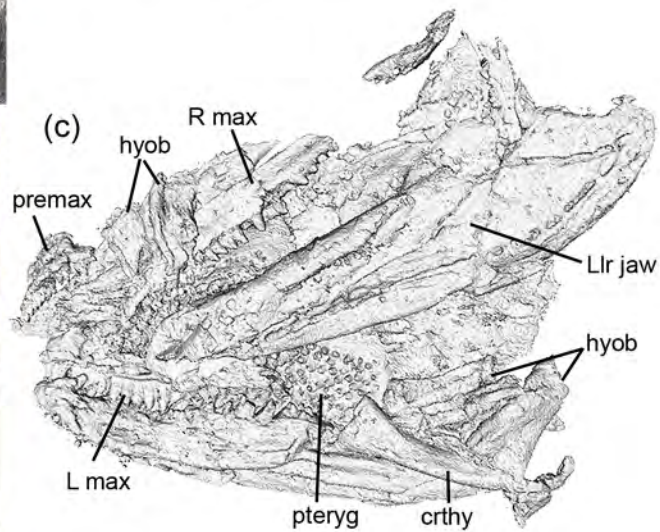
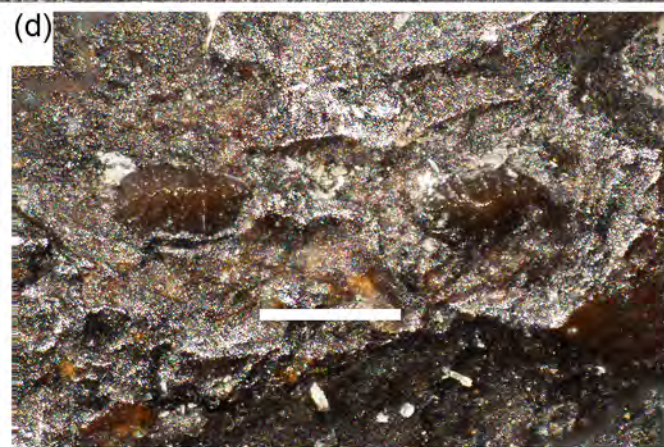
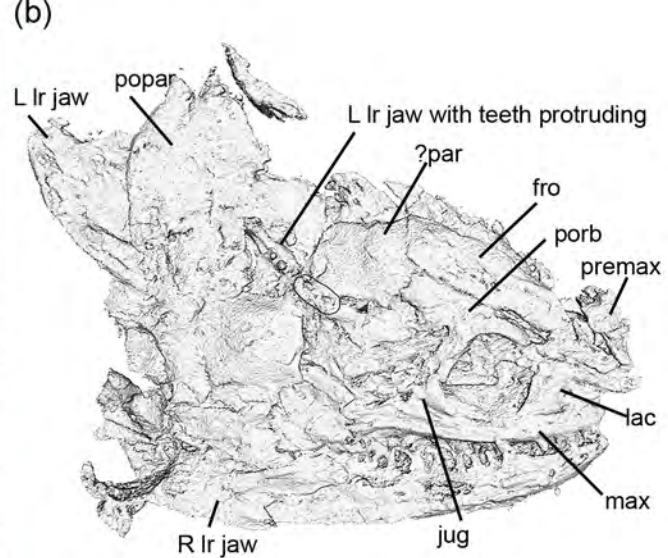
509

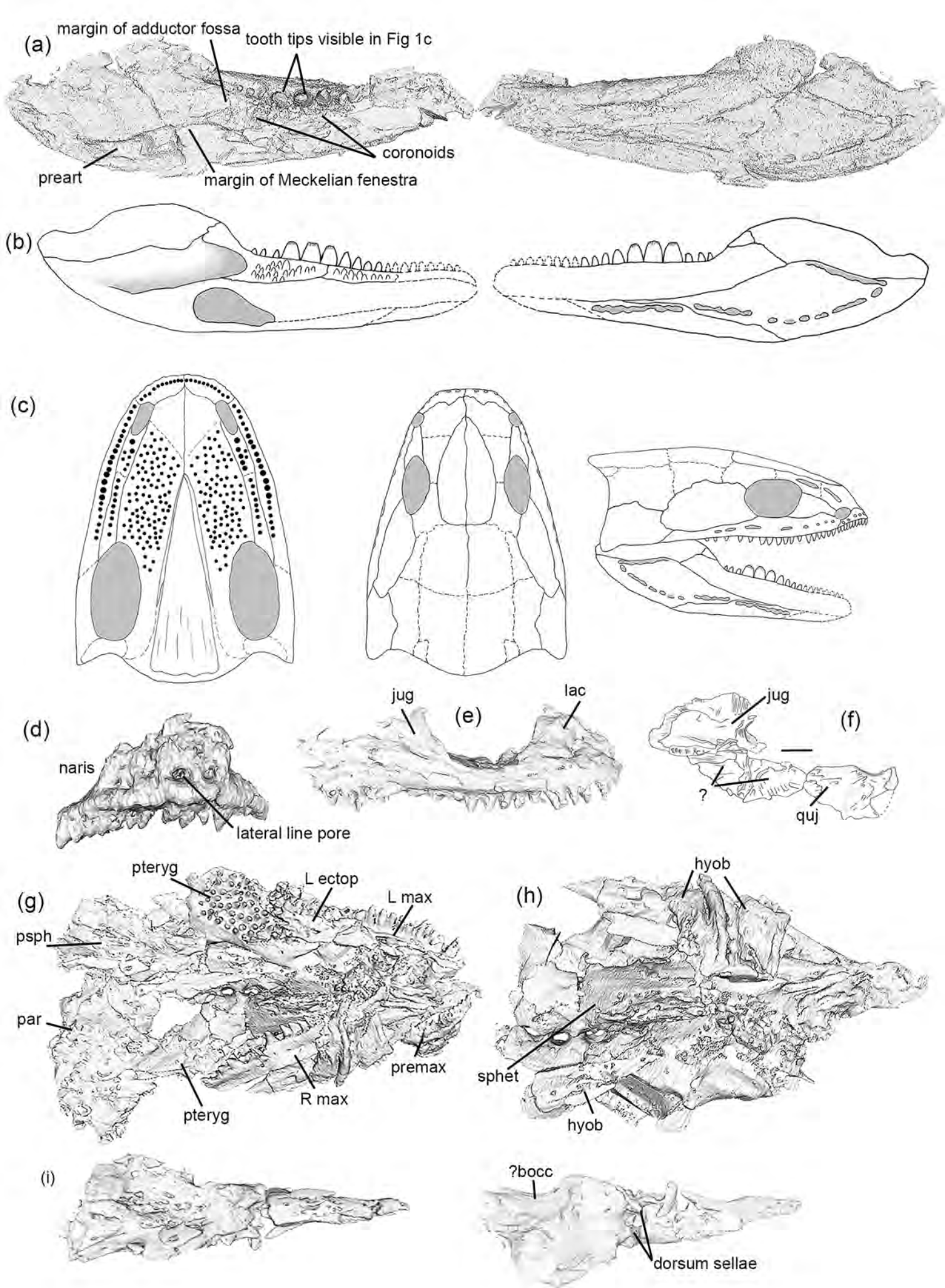
510

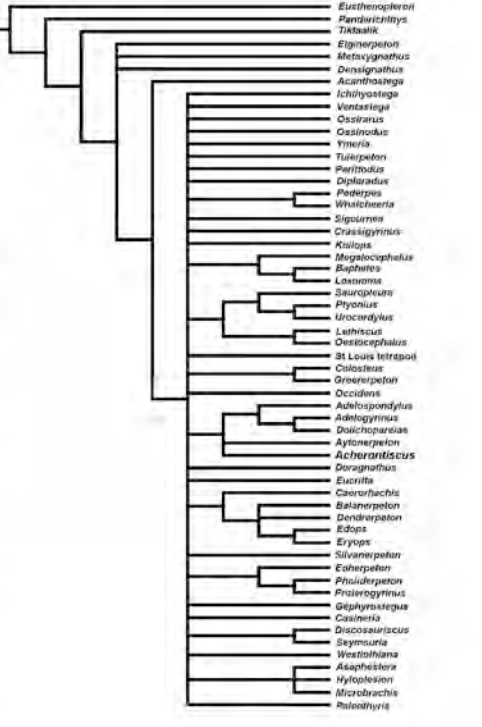
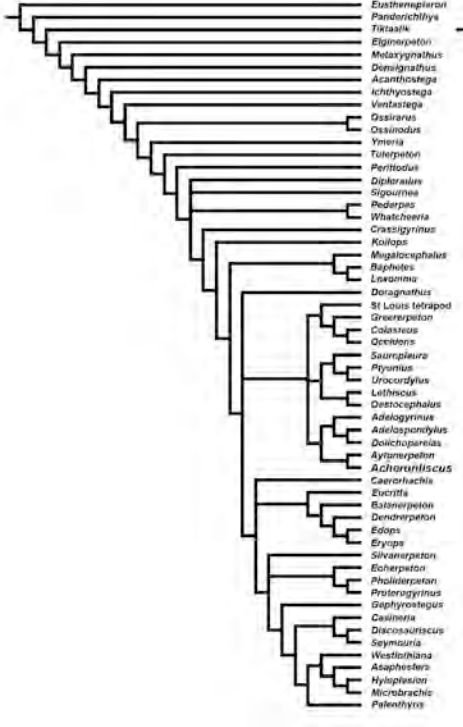
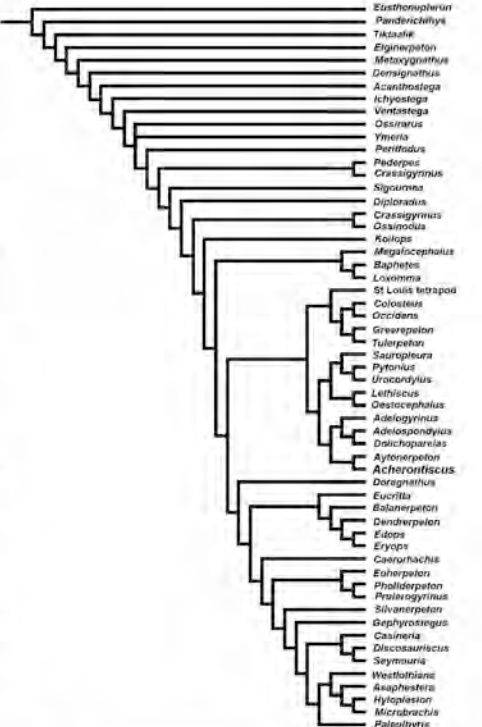
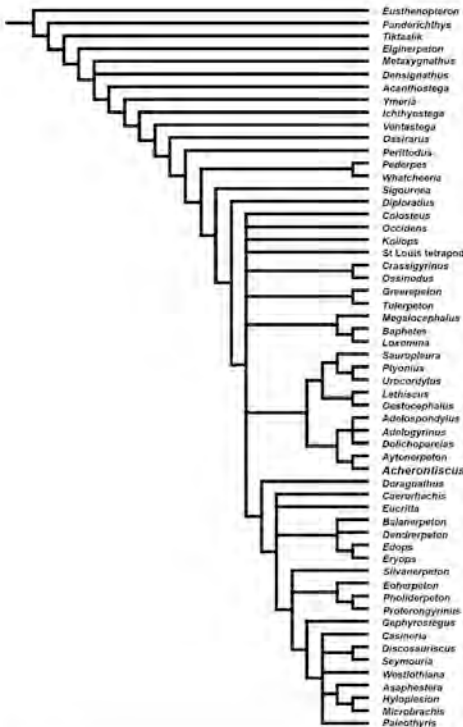
511

512

513









## Electronic Supplementary Material

### S1 Palynological analysis

#### The age and environment of *Acherontiscus*

##### Materials and Methods

Two samples (Ach-1 and Ach-2) were supplied from the matrix of *Acherontiscus*. These weighed 0.1g and <0.1g respectively. These were surface inspected for any likely contamination or evidence of specimen stabilisation during curation and conservation. Both appeared to be clean fragments of the matrix. Importantly they represent single laminae from the rock sample as opposed to composites of the entire sample. Given the small size of the samples they were processed on a small scale using screw topped Savillex™ PFA digestion vessels and small sieves to preserve the residue and prevent any contamination. Initially they were treated uncrushed with 60% HF for 16 hours. But the samples failed to disaggregate on account of the high organic matrix. So, they were decant washed clean of HF and then subjected to 15 hours in fuming nitric acid. Ach-2 disaggregated readily but the matrix of Ach-1 failed to dissolve so was crushed down to sub-mm size and then returned to fuming nitric acid for a further 15 hours which proved to be successful. The residues were diluted in water and then sieved at 15 µm to concentrate the spores. At this point both samples contained residual mineral including mica and so were returned to the digestion vessels for 12 hours in 60% HF and resieved at 15 µm before storage in a vial. Multiple slides of the very small amount of residue was then mounted using Elvacite 2044™ to produce one sparse, poorly preserved but workable palynological assemblage from Ach-1 and a better assemblage from Ach-2.

##### Age of the *Acherontiscus* matrix

The specimen was initially dated by AHV Smith who was a palynologist with the then National Coal Board. He applied the palynological scheme devised by Coal Board palynologists (Smith & Butterworth, 1967) for determining the age of coal samples. Smith reported a rich palynological assemblage that included *Cingulizonates* cf. *capistratus*, *Rotaspora knoxae* and *Tripartites trilinguis* in addition to other taxa that were not specified in the report in Carroll (1969). This placed the sample in their Assemblage III (upper Lower Limestone Group to upper Limestone Group and including the Limestone Coal Group) with an age range (Fig. 1) of late Viséan to mid Namurian. It is timely to revisit this age assignment given that there are new zonal schemes available which include considerably more information available on the ranges of Carboniferous spores and particularly in non-coal lithologies. These more recent zonal schemes are based around sections in northern England and Scotland and include Neves *et al.*, 1972; Owens *et al.* 1977; Clayton *et al.*, 1977; Brindley & Spinner 1989; Owens *et al.*, 2004; 2005 together with information from the compilation by Butterworth (1984). Spore zones and ranges of key taxa are shown on Fig. 1.

The assemblages from the 2 samples (Table 1, Plate 1) are strikingly different, Ach-1 being dominated by *Cingulizonates* cf. *capistratus* with *Botryococcus* whereas Ach-2 is dominated by *Lycospora* spp. This is interpreted as a consequence of separately analysing single laminae rather than a homogenized bulk sample. The single laminae represent distinctly different depositional episodes with distinctly different palynological inputs. A key element in both assemblages are spores with distinct radial extensions. These include *Tripartites vetustus* together with *Rotaspora* (*R. fracta* and *R. knoxae*) which all have inceptions in the latest Viséan Brigantian stage. This is confirmed by the presence of late Brigantian or younger taxa that include abundant *Cingulizonates* cf. *capistratus* together with *Reticulatisporites carnosus*, *Triquitrites trivalvis* and *Tripartites trilinguis* which define the Cc zone. An addition

constraint is the presence of very rare larger pollen grains (*Florinites* spp) which also have an inception in the latest Brigantian (Clayton, 1996). The combined ranges of these taxa (Fig. 1) give a total age range of latest Brigantian to Arnsbergian. However, a key but very rare species is *Verrucosisporites morulatus* for which 3 complete specimens are present together with other fragments. This spore is characterized by its distinctive sculpture of rounded verrucae that are irregular in size and hence irregularly spaced. This single taxon defines the *Verrucosisporites morulatus* or Vm subzone (Owens *et al.*, 2004) which has its base at approximately the Viséan-Namurian boundary and its top at the E<sub>1</sub>-E<sub>2</sub> ammonoid sub-zone boundary with is also marked by the last occurrence of *Reticulatisporites carnosus*. This makes *Acherontiscus* Pendleian (earliest Namurian) in age. In terms of lithostratigraphy within the Midland Valley rare goniatites (Ramsbottom 1977) show the Pendleian to be between the Top Hosie (i.e. the Great Limestone of northern England) and Orchard Limestone. This includes the Limestone Coal Group and the lower part of the Upper Limestone Group and includes the ironstones that are the likely stratigraphic level for the *Acherontiscus* specimen.

Given the Pendleian date for *Acherontiscus* it is most likely to have been collected from the Borough Lee Ironstone at Loanhead. This was an active coal mining area south of Edinburgh during the 1880s yielding many vertebrate fossils representing a very diverse fauna.

### **Palaeoenvironment of the *Acherontiscus* sample**

The two different samples give quite different palaeoenvironments that show the range of likely habitats in which the *Acherontiscus* specimen was found. Ach-1 is dominated by *Botryococcus* which is a fresh water alga that lives today in still fresh water ponds and lakes. This abundance implies that *Acherontiscus* was living in and around a small lake. *Cingulizonates* cf. *capistratus* (as *Cingulizonates bialatus*) is known *in situ* from *Porostrobis*, a herbaceous lycopod (Bek & Leary, 2012) from which we can infer that the lake was surrounded by a stand of lower vegetation. There was local run off into the lake, i.e. more than a rainfall fed system, as shown by the minor clastic component of clay minerals and mica that remained in the samples following oxidation. However, a dominance of such cingulate microspores is generally interpreted (Bek & Leary, 2012) as signifying an environment that is less wet than a coal swamp. *Vestispora* is also present which is a distinct spore with a circular operculum and originates (Balme, 1995) from the horse-tail equisetitalean relative *Bowmanites* showing these to be present in the flora.

Ach-2 was quite different in being dominated by *Lycospora* spp., largely *L. noctuina*. This belongs to the *Lycospora uber* group (Bek, 2012) and are cones of the arborescent lycopod *Lepidodendron*. During deposition of this lamina the flora was dominated by larger lycopods and more typical of a coal swamp vegetation.

The original sample studied by Smith was dominated by *Cingulizonates* cf. *capistratus*. This was prepared in the labs of the NCB and would normally have been a significantly sized sample (1g in Smith & Butterworth, 1967) that would have integrated the laminations in the sample. This suggests that the local palaeoenvironment was more likely herbaceous lycopods surrounding a small freshwater lake.

- Balme, B.E. 1995. Fossil in situ spores and pollen grains: an annotated catalogue. *Review of Palaeobotany and Palynology*, 87, 81-323
- Bek, J. & Leary, R.L. 2012. *Porostrobis nathorstii* (Leary & Mickle) emend. and its spores from the Namurian of Illinois, USA. *Bulletin of Geosciences*, 87, 45-52.
- Bek, J. 2012. A review of the genus *Lycospora*. *Review of Palaeobotany and Palynology*, 174, 122-135.

- Brindley & Spinner 1989. Palynological assemblages from Lower Carboniferous deposits, Burntisland district, Fife, Scotland. *Proceedings of the Yorkshire Geological Society*, 47, 215-231.
- Butterworth, M. 1984. Upper Carboniferous. *Pollen and spore biostratigraphy of the Phanerozoic in North-West Europe*. BMS Palynology Group Meeting, Cambridge 1984.
- Clayton, G. 1996. Mississippian spores. In: Jansonius, J. & McGregor, D.C. (eds) *Palynology: principles and applications*, American Association of Stratigraphic Palynologists Foundation, 2, 589-596.
- Clayton, G., Coquel, R., Doubinger, J., Gueinn, K.J., Loboziak, S., Owens, B. & Streel, M. 1977. Carboniferous miospores of Western Europe: illustration and zonation. *Mededelingen Rijks Geologische Dienst*, 29, 1-71.
- Owens, B., McLean, D & Bodman, D. 2004. A revised palynozonation of British Namurian deposits and comparisons with eastern Europe. *Micropalaeontology*, 50, 89-103.
- Owens, B., Neves, R., Gueinn, K.J., Mishell, D.R.F., Sabry, H.S.M.Z. & Williams, J.E. 1977. Palynological division of the Namurian of northern England and Scotland. *Proceedings of the Yorkshire Geological Society*, 41, 381-398.
- Neves, R., Gueinn, K.J., Clayton, G., Ioannides, N.S., Neville, R.S.W. & Kruszkowska, K. 1973. Palynological correlations within the Lower Carboniferous of Scotland and Northern England. *Transactions of the Royal Society of Edinburgh*, 69, 23-70.
- Owens, B., McLean, D., Simpson, K.R.M., Shell, P.M.J. & Robinson, R. 2005. Reappraisal of the Mississippian palynostratigraphy of the East Fife coast, Scotland. *Micropalaeontology*, 50, 89-103.
- Ramsbottom, W.H.C. 1977. Correlation of the Scottish Upper Limestone Group (Namurian) with that of the North of England. *Scottish Journal of Geology*, 13, 327-330.
- Smith, A.H.V. & Butterworth, M.A. 1967. Miospores in the coal seams of the Carboniferous of Great Britain. *Special Papers in Palaeontology*, 1, 1-324.

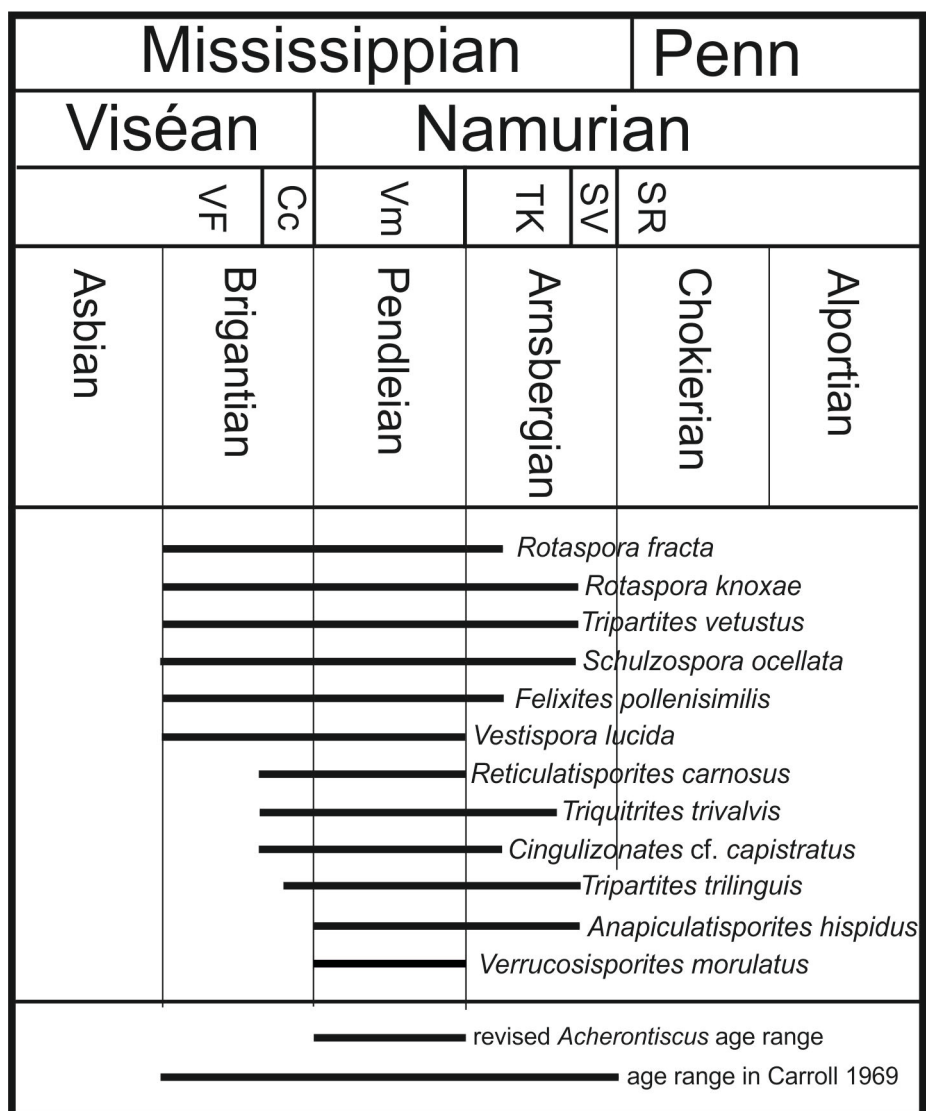


Figure S2. Range chart of spore taxa occurrences for age estimation of *Acherontiscus*.



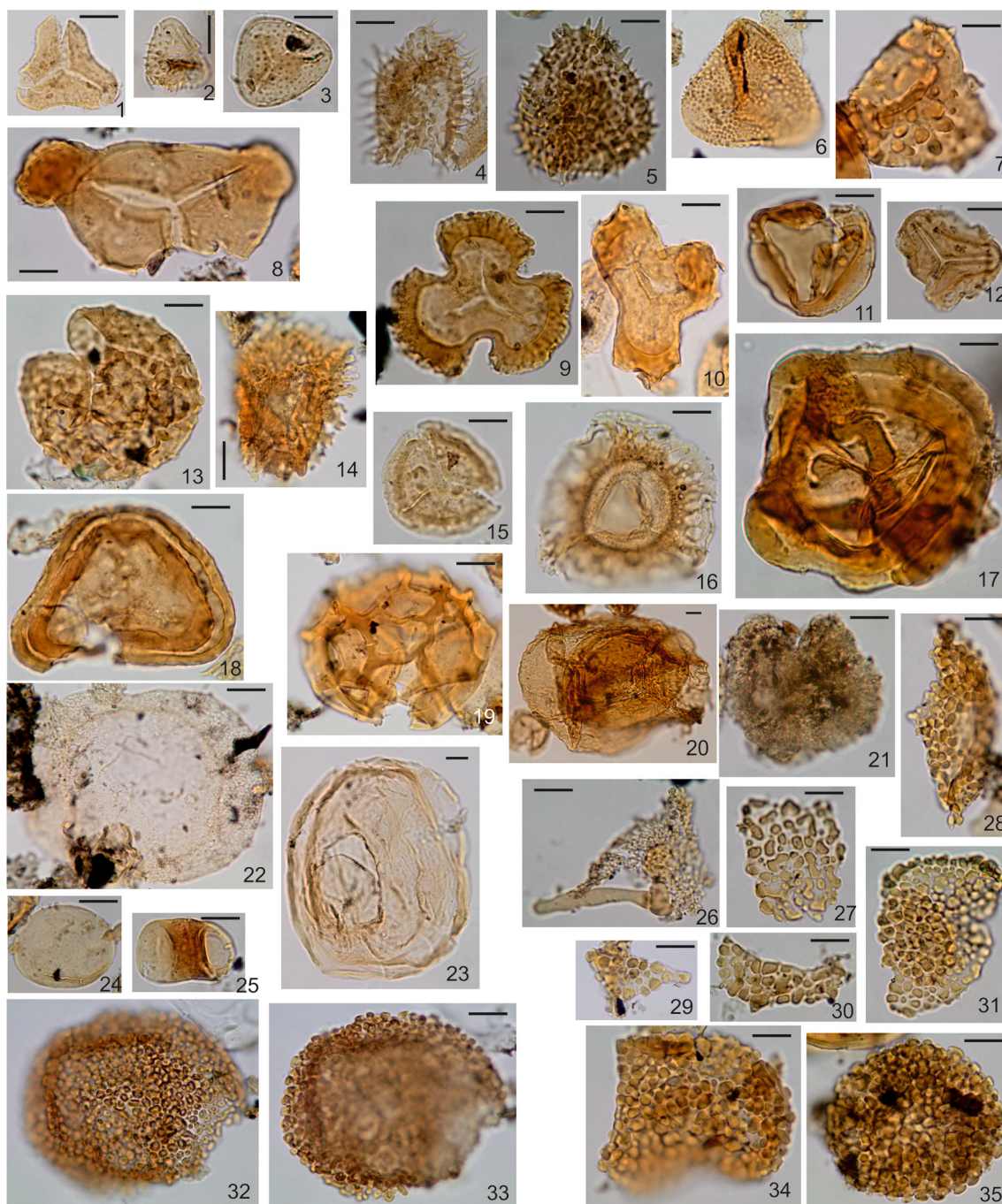


Figure S2. All illustrated palynomorphs and slides are curated in the collections of the NMS, Scotland. They will be linked to NMS G. 1967.13.1 *Acherontiscus caledoniae*. The slide co-ordinates are for Olympus BHS-313 210685 and England Finder co-ordinates (e.g., K15-2 ) are supplied. All scale bars are 10 µm.

1. *Waltzispora planiangularata* Ach-2.2 (127.5, 4.2), Y27-1.
2. *Anapiculatisporites hispidus* Ach-2 (121.4, 14), O21-1.
3. *Anapiculatisporites concinnus* Ach-2 (114.6, 15.9), M14-1.
4. *Acanthotriletes acritarchus* Ach-2.2 (135.7, 13), P35-1.
5. *Acanthotriletes hastatus* Ach-2.2 (126.2, 22.4), E26-1.
6. *Tricidarispores arcuatus* Ach-2 (126.8, 6.9), V26-4.
7. *Pustulatisporites papillosus* Ach-2 (116.5, 10.4), R16-3.
8. *Triquitrites trivalvis* Ach-2 (128, 7.1), V27-2.

9. *Tripartites trilinguis* Ach-1.4 (133.1, 17.1), K33-3.
10. *Tripartites vetustus* Ach-2.2 (126.2, 19.9), H26-1.
11. *Rotaspora knoxae* Ach-2.2 (123.8, 11.1), R23-2.
12. *Rotaspora fracta* Ach-2 (116.1, 18), K15-2.
13. *Grumosisporites* Ach-2 (132, 18.1), J32-3.
14. *Cristatisporites indignabundus* Ach-2 (117.1, 5.8), W16-4.
15. *Lycospora noctuina* Ach-2.2 (128, 18.1), J28-3.
16. *Cingulizonates* cf. *capistratus* Ach-1.1 (128.2, 13.5), O28-3.
17. *Reticulatisporites carnosus* Ach-2 (126, 19.2), H25-4.
18. *Simozonotriletes intortus* Ach-2 (123.6, 23), D23-3.
19. *Reticulatisporites reticulatus* Ach-2 (117.5, 10), S17-1.
20. *Remysporites magnificus* Ach-2.4 (133, 8.5), T33-3.
21. *Botryococcus* Ach-1.1 (128, 22), E28-3.
22. *Schulzospora ocellata* Ach-1.1 S (136.5, 6.8), V36-4.
23. *Vestispora lucida* Ach-1.2 (124.4, 13.7), O24-1.
24. *Laevigatosporites minor* Ach-2.2 (129.2, 13.2), P29-1.
25. *Felixites pollenisimilis* Ach-2 (128.4, 10), S28-1.
26. Lycopod megaspore fragment Ach-1.1 (130, 20), G29-4.
27. *Verrucosisporites morulatus* Ach-2.2 (127.9, 9.2), T27-2.
28. *Verrucosisporites morulatus* Ach-2 (126, 19.2), H25-4.
29. *Verrucosisporites morulatus* Ach-2.3 (123.1, 7.9), U22-2.
30. *Verrucosisporites morulatus* Ach-1.4 (128.4, 10.4), R28-3.
31. *Verrucosisporites morulatus* Ach-2 (129.4, 12), Q29-1.
32. *Verrucosisporites morulatus* Ach-2.3 (130.7, 14.9), N30-2.
33. *Verrucosisporites morulatus* Ach-2.3 (130.7, 14.9), N30-2.
34. *Verrucosisporites morulatus* Ach-2.3 (116, 11.8), Q15-4.
35. *Verrucosisporites morulatus* Ach-1.4 (126.2, 18.8), J26-1.

Table 1 Palynomorphs from the matrix of *Acherontiscus*. All taxonomic citations are in Owens *et al.*, (2004) or Brindley & Spinner (1989).

	Ach-1	Ach-2
<i>Acanthotriletes acritarchus</i>		+
<i>Acanthotriletes castanea</i>		+
<i>Acanthotriletes hastatus</i>		+
<i>Anapiculatisporites concinnus</i>		+
<i>Anapiculatisporites hispidus</i>		+
<i>Calamospora</i> spp		+
<i>Cingulizonates</i> cf. <i>capistratus</i>	30%	+
<i>Cristatisporites indignabundus</i>		+
<i>Felixites pollenisimilis</i>		+
<i>Florinites</i> spp		+
<i>Grumosisporites</i> sp		+
<i>Laevigatosporites minor</i>		+
<i>Leiotriletes politus</i>	+	
<i>Lycospora noctuina</i>		+
<i>Lycospora</i> spp	+	53%
<i>Mooreisporites</i> sp		+
<i>Pustulatisporites papillosus</i>		+
<i>Remysporites magnificus</i>		+
<i>Reticulatisporites carnosus</i>	+	

<i>Rotaspora fracta</i>		+
<i>Rotaspora knoxae</i>		+
<i>Schulzospora campyloptera</i>		+
<i>Schulzospora ocellata</i>	+	
<i>Simozonotriletes intortus</i>	+	
<i>Triquitrites marginatus</i>	+	
<i>Tricidarisorites arcuatus</i>		+
<i>Tripartites trilinguis</i>		+
<i>Tripartites vetustus</i>	+	
<i>Triquitrites trivalvis</i>	+	+
<i>Verrucosisporites morulatus</i>	+	+
<i>Vestispora lucida</i>	+	
<i>Waltzisporea planiangularata</i>		+
Megaspore (lycopod)	+	
Botryococcus	37%	+

**S2 Dryad storage includes:** three movies; *Acherontiscus* left lower jaw removed (6.6MB), *Acherontiscus* left lower jaw (2.5 MB), and *Acherontiscus* skull roof (4.2MB), and the micro-CT scan data.

### S3 Phylogenetic Analyses, Character List and Data matrix

**Database construction.** The 12 taxa added to the matrix of Clack et al. 2017: *Acherontiscus*; the stem-group tetrapods *Elginerpeton* (Ahlberg, 1995, 1998) and *Densignathus* (Daeschler 2000); an unnamed colosteid-like tetrapod from the St. Louis Limestone, Missouri, USA (Clack et al. 2012); three adelospondyls (*Adelogyrinus*; *Adelospondylus*; *Dolichopareias* (Carroll et al. 1998); two aïstopods (*Lethiscus*; *Oestocephalus* (Anderson 2003, Pardo et al. 2017); three nectrideans (*Sauroplorea*; *Ptyonius*; *Urocordylus* (Carroll et al. 1998).

**Parsimony methods.** All parsimony analyses were run under identical search settings in PAUP\* v. 4.0a164 (Swofford 2003). *Eusthenopteron* was chosen as an outgroup to polarize characters. In all cases, the “amb-” option was enforced, whereby branches were collapsed into polytomies if they had a minimum length of zero. All instances of multistate coding were treated as uncertainties, and all multistate characters were left unordered. Only two characters were uninformative. Given the size of the matrix, heuristic tree search methods were employed. To explore as much of the tree landscape as possible, and to prevent PAUP\* from getting stuck in local tree island optima, an initial round of heuristic searches was carried out with 5000 random stepwise taxon addition sequence replicates, holding a single tree in memory at each replicate, and using the tree bisection-reconnection algorithm for branch swapping. After this round, five consecutive branch-swapping searches were applied to the trees retained in memory, this time with the option of holding multiple trees. Neither additional nor shorter trees resulted from these additional search rounds in any of the parsimony analyses.

In the case of analyses that produced several equally parsimonious trees, two filtering criteria were applied, as follows: only binary (i.e., fully bifurcated) trees were kept; if a non-binary tree was compatible with a binary tree then the non-binary tree was discarded. Only trees that satisfied these filtering criteria were kept in memory. Conflicting topologies in the most parsimonious filtered trees were summarized with three consensus methods (strict; 50% majority-rule; Adams) and with a maximum agreement subtree (i.e., a pruned tree including the largest subset of taxa that exhibit identical mutual relationships in all trees) (figure S3).

Parsimony analyses were run under three different character weighting schemes, namely: all characters having equal unit weights (unweighted analysis); all characters reweighted by the maximum value of their rescaled consistency index from the unweighted analysis; implied weighting (Goloboff 1993). Under implied weighting, we experimented with different integer values of the  $K$  constant of concavity, specifically  $1 \leq K \leq 10$ . Trees obtained from all the implied weighting analyses were collated in PAUP\*, and nodes common to all the  $K$ -weighted topologies were summarised with a strict, 50% majority-rule, and Adams consensus, as well as with an agreement subtree (Congreve and Lamsdell 2016).

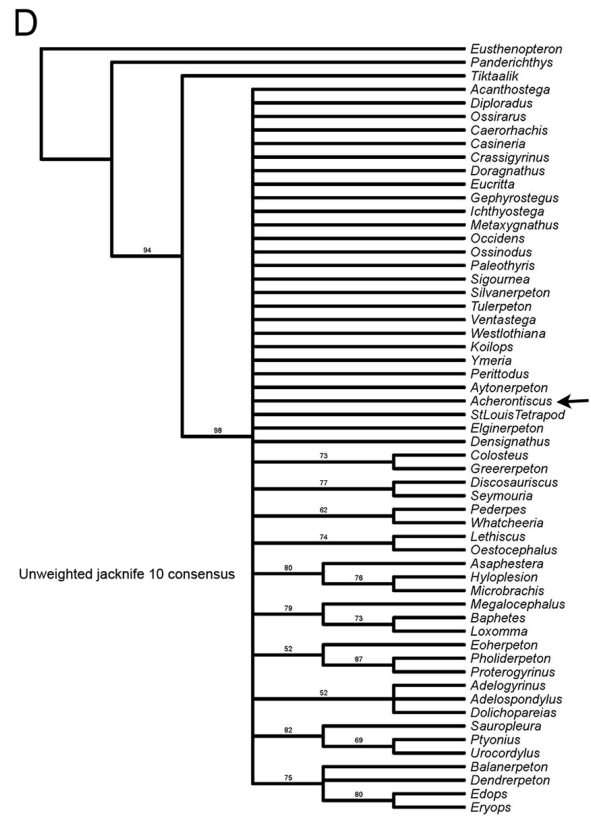
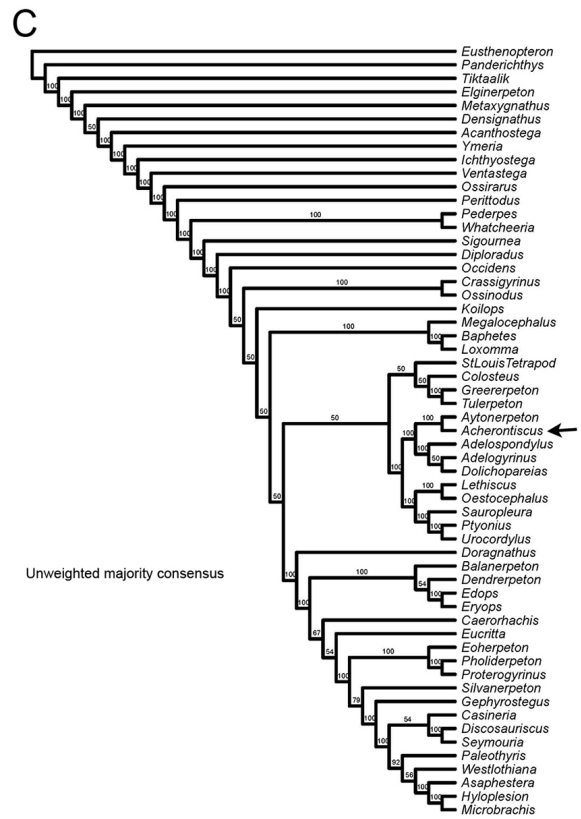
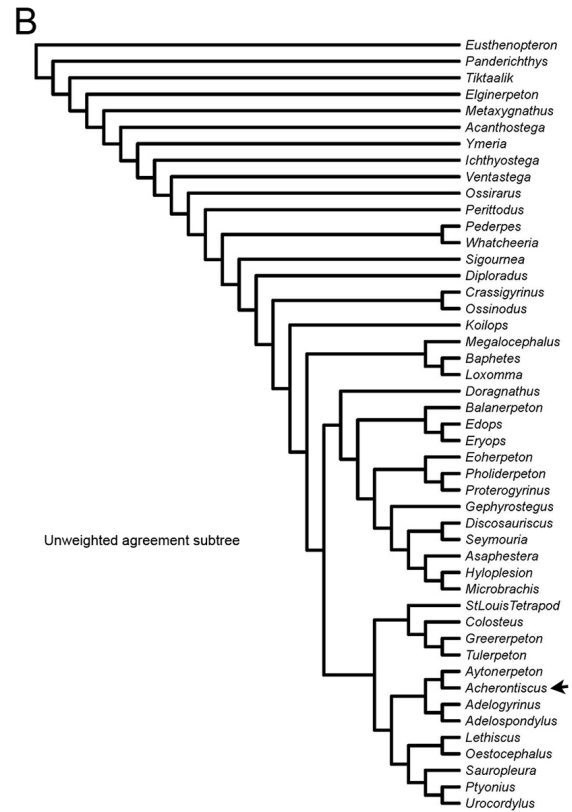
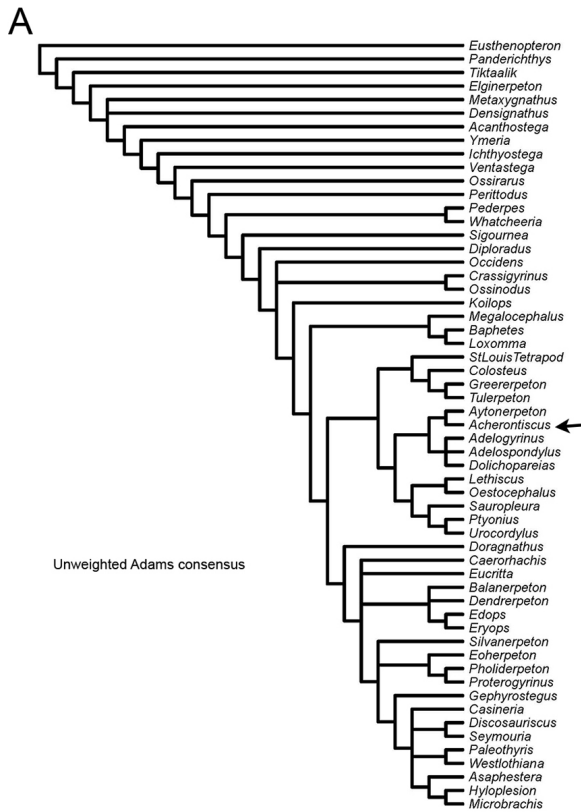
Statistical support for tree nodes was assessed in two ways. Firstly, we carried out a bootstrap analysis of the data matrix (Felsenstein 1985) with 5000 random character resampling replicates, using the fast stepwise-addition option, and resampling the full set of characters. Bootstrap percentage support was shown on a 50% majority-rule consensus that retained only those groups for which support was greater than 50%. Secondly, we performed jackknifing (Farris et al. 1996), once again with 5000 random character resampling replicates under the fast stepwise-addition option. To evaluate the effects of different proportions of character deletion on node support, nine jackknifing analyses were undertaken with increments of 10% in character deletion, (i.e., 10%, 20%, 30%, ... 90% of all characters were eliminated at random, and node support was calculated at the end of each round of deletions).

**Bayesian methods.** A Bayesian inference analysis was carried out in MrBayes v. 3.2.6 (Ronquist and Huelsenbeck 2003), with the following settings: variable coding; gamma-distributed rate model;  $10^7$  generations and four chains; discarding the first 25% of sampled trees. Convergence diagnostic was evaluated through inspection of the Potential Scale Reduction Factor values (Gelman and Rubin 1992) output by MrBayes.

- Ahlberg P.E. 1995 *Elginerpeton pancheni* and the earliest tetrapod clade." *Nature* 373, 420-425.
- Ahlberg, P.E. 1998. "Postcranial stem tetrapod remains from the Devonian of Scat Craig, Morayshire, Scotland." *Zoological Journal of the Linnean Society* 122: 99-141.
- Daeschler, E.B. 2000. "Early tetrapod jaws from the late Devonian of Pennsylvania, USA." *J. Paleont.* 74 (2), 301-308.
- Clack, J.A., Witzmann, F., Müller, J. and Snyder, D., 2012. A colosteid-like early tetrapod from the St. Louis Limestone (Early Carboniferous, Meramecian), St. Louis, Missouri, USA. *Fieldiana Life and Earth Sciences*, pp.17-39.
- Carroll RJ, Bossy, KA, Milner AC, Andrews SM, Wellstead CF. 1998 *Lepospondyli: Handbook of Paleoherpertology*, Part 1. Munich, Germany: Verlag Dr Friedrich Pfeil.
- Anderson JS. 2003. Cranial anatomy of *Coloraderpeton brilli*, postcranial anatomy of *Oestocephalus amphiuminus*, and reconsideration of Ophiderpetontidae (Tetrapoda: Lepospondyl: Aistopoda). *J. Vertebr. Paleont.* 23, 532-543.
- Pardo JD, Szostakiwskyj M, Ahlberg PE and Anderson JS. 2017 Hidden morphological diversity among early tetrapods. *Nature* 546, 642-645
- Swofford, D. L. 2003. PAUP\*. Phylogenetic Analysis Using Parsimony (\*and other methods). Version 4. Sinauer Associates, Sunderland, Massachusetts
- Goloboff, P. A. 1993. Estimating character weights during tree search. *Cladistics*. 9: 83–91
- Congreve, C. R., & Lamsdell, J. C. 2016. Implied weighting and its utility in palaeontological datasets: a study using modelled phylogenetic matrices. *Palaeontology*, 59(3), 447-462.
- Felsenstein, J. 1985. Confidence limits on phylogenies: An approach using the bootstrap. *Evolution* 39:783–791.
- Farris, J. S., V. A. Albert, M. Källersjö, D. Lipscomb, A. G. Kluge. 1996. Parsimony jackknifing out- performs neighbor-joining. *Cladistics* 12, 99–124

- Ronquist, F. and J. P. Huelsenbeck. 2003. MRBAYES 3: Bayesian phylogenetic inference under mixed models. *Bioinformatics* 19,1572-1574.
- Gelman, A. and Rubin, D.B. 1992. Inference from iterative simulation using multiple sequences. *Statistical science*, 7 (4), pp.457-472.

Fig. 3. Interrelationships of major group of early tetrapods, additional cladistic experiments. A Adams consensus; B agreement subtree; C 50% majority-rule consensus of 312 equally parsimonious trees with unweighted characters. The proportions of all most parsimonious trees, greater than or equal to 50 percent, that show the relevant nodes to which the numbers refer and including groupings that are compatible with that consensus; D jackknife node support values based on 5000 random resampling replicates of half of the characters.





### Skull roof and braincase

1. Anterior tectal (accessory dermal bone associated with naris having surface ornament and absent lateral line canal; treated here as septomaxilla): present = 0, absent = 1
2. Anterior tectal: narial opening ventral to it = 0; narial opening anterior to it = 1
3. Basioccipital: indistinguishable from exoccipitals = 0, separated by suture = 1
4. Basioccipital: ventrally exposed portion longer than wide = 0, shorter than wide = 1
5. Basioccipital: condyle: absent, notochordal = 0; present = 1
6. Basispterygoid junction: basispterygoid process fits into socket recessed into epipterygoid = 0, pterygoid/epipterygoid forms narrow bar or process that clasps basispterygoid process = 1
7. Exoccipitals: meet skull table: absent = 0, present = 1
8. Exoccipital contributes to condyle: absent = 0, present = 1
9. Exoccipitals enlarged to form double horizontally orientated occipital condyle, (may exclude basioccipital from articular surface): absent = 0, present = 1
10. Frontal – parietal length ratio: frontals shorter = 0, longer = 1, subequal = 2
11. Frontal anterior margin wedged between nasals: absent = 0, present = 1
12. Frontal – nasal length ratio: frontals approximately equal to or less than one-third as long as nasals = 0, more than one-third as long = 1
13. Intertemporal present: present = 0, absent = 1
14. Intertemporal smaller than supratemporal = 0, or larger than/comparable in size with supratemporal = 1.
15. Intertemporal lateral edge: not interdigitating with cheek = 0, interdigitates = 1
16. Intertemporal contacts squamosal: absent = 0, present = 1
17. Jugal deep below orbit (vs narrow process): 50% - > 50% orbit diam = 0, <50% = 1
18. Jugal contribution to orbit margin: less than one-third = 0, equal to or more than one-third = 1
19. Jugal alary process on palate: absent = 0, present = 1
20. Jugal length of postorbital region relative to one-third of the length of the postorbital cheek region: greater = 0 or less = 1
21. Jugal extends anterior to anterior orbit margin: absent = 0, present = 1
22. Jugal not interposed between maxilla and quadratojugal thus not contributing to skull lower margin = 0 or interposed = 1.
23. Jugal V-shaped indentation of posterodorsal margin: absent = 0, present = 1
24. Lacrimal contributes to narial margin: absent, excluded by anterior tectal = 0; present = 1, absent, excluded by nasal/maxillary or prefrontal/maxillary suture = 2
25. Lacrimal reaches orbit margin (= prefrontal/ jugal suture): present = 0, absent = 1
26. Maxilla sutures to vomer: absent = 0, present = 1
27. Maxilla external contact with premaxilla: narrow contact point not interdigitated = 0, interdigitating suture = 1
28. Maxilla highest point in posterior half = 0, anterior third of its length = 1, or at its midlength = 2
29. Maxilla extends behind level of posterior margin of orbit: present = 0, absent = 1
30. Maxilla sutures to prefrontal: absent = 0, present = 1
31. Maxilla – premaxilla contact shelf-like mesial to tooth row on palate: absent = 0, present = 1
32. Median rostral (=internasal): mosaic = 0, paired = 1, single = 2, absent = 3
33. Nasals contribute to narial margin: absent = 0, present = 1

34. Nasal – parietal length ratio less than 1.45 = 0 or greater than 1.45 = 1
35. Nasal smaller in area than postparietal: absent = 0, present = 1
36. Opisthotic paroccipital process ossified and contacts tabular below post-temporal fossa: absent = 0, present = 1, post-temporal fenestra absent = 2
37. Opisthotic forms substantial plate (with supraoccipital if present) beneath skull table: present = 0, absent = 1
38. Parietal meets tabular: absent = 0, present = 1
39. Parietal – postorbital suture: absent = 0, present = 1
40. Parietal anterior portion extent relative to orbit midlength: in front of = 0, level with = 1, posterior to = 2
41. Parietal shape of anteriormost third: not wider than frontals = 0, at least marginally wider = 1
42. Parietal – postparietal suture strongly interdigitated: absent = 0, present = 1
43. Postfrontal – prefrontal contact: broad = 0; or point-like = 1
44. Postfrontal – prefrontal suture: anterior half of orbit = 0, middle or posterior half of orbit = 1, absent = 2
45. Postorbital suture to skull table (intertemporal or supratemporal) interdigitating vs smooth: smooth = 0, interdigitating = 1
46. Postorbital without distinct dorsomedial ramus for postfrontal = 0, with incipient ramus = 1, with elongate ramus = 2
47. Postorbital shape: irregularly polygonal = 0, broadly crescentic and narrowing to a posterior point = 1
48. Postorbital longer than anteroposterior width of orbit: absent = 0, present = 1
49. Postorbital at least one quarter of the width of the skull table at the same transverse level: absent = 0, present = 1
50. Postparietal: longer than wide = 0, approximately square or pentagonal = 1, wider than long = 2
51. Postparietal occipital flange exposure: absent = 0, present = 1
52. Postparietal – exoccipital suture: absent = 0, present = 1
53. Prefrontal less than three times longer than wide: present = 0, more than, = 1.
54. Prefrontal enters naris: absent = 0, present = 1
55. Prefrontal contributes to half or more than half anteromesial orbit margin = 0, less than half = 1
56. Premaxilla posterodorsal alary process onto snout: absent = 0, present = 1
57. Premaxilla forms part of choanal margin: broadly = 0, point = 1, not, excluded by vomer = 2
58. Preopercular present = 0, absent = 1
59. Squamosal posterodorsal margin shape: convex = 0, sigmoid or approximately straight = 1, entirely concave = 2
60. Squamosal contact with tabular: smooth = 0, interdigitating = 1, absent = 2
61. Squamosal suture with supratemporal position: within skull table = 0, at apex of temporal embayment = 1, dorsal to apex = 2, ventral to apex = 3, absent = 4
62. Squamosal anterior part lying behind mid-parietal length: present = 0, absent = 1
63. Squamosal interdigitating suture with supratemporal: absent = 0, present = 1
64. Squamosal contacts tabular on dorsal surface of skull: absent = 0, present = 1
65. Supratemporal present as a separate ossification: present = 0, absent = 1
66. Supratemporal forms part of skull margin posteriorly: absent = 0, present = 1
67. Tabular lateral horn (subdermal unornamented component): absent = 0, button = 1, blade = 2
68. Tabular prolonged posterolateral ornamented surface absent = 0, present = 1



- 69. Tabular emarginated lateral margin: absent = 0, present = 1
- 70. Tabular occipital flange exposure: absent = 0, extends as far ventrally as does postparietal = 1, extends further ventrally than does postparietal = 2

#### Palate

- 71. Ectopterygoid as long or longer than palatines: present = 0, absent = 1
- 72. Ectopterygoid reaches subtemporal fossa: absent = 0, present = 1
- 73. Ectopterygoid – palatine exposure: more or less confined to tooth row = 0, broad mesial exposure additional to tooth row = 1
- 74. Lateral rostral present: present = 0, absent = 1
- 75. Parasphenoid grooved ventrally about half of length = 0, vs narrow V-shaped section cultriform process along whole length = 1, flat and more or less broad = 2
- 76. Parasphenoid cultriform process shape in ventral view: biconvex = 0, narrowly triangular = 1, parallel-sided = 2, or with proximal constriction followed by swelling = 3
- 77. Parasphenoid depression in body: absent = 0, single median = 1, double = 2
- 78. Parasphenoid posterolateral wings (ridged): absent = 0, present = 1
- 79. Parasphenoid wings: separate = 0, joined by web of bone = 1
- 80. Parasphenoid contacts or sutures to vomers: present = 0, absent = 1
- 81. Parasphenoid carotid grooves: curve round basiptyergoid process = 0, lie posteromedial to basiptyergoid process (or enter via foramina there) = 1, absent = 2
- 82. Parasphenoid/basisphenoid ventral cranial fissure: not sutured = 0, sutured but traceable = 1, eliminated = 2
- 83. Pterygoids separate in midline = 0, meet in midline anterior to cultriform process = 1
- 84. Pterygoids flank parasphenoid for most of length of cultriform process; present = 0, absent = 1
- 85. Pterygoid quadrate ramus margin in adductor fossa: concave = 0, with some convex component = 1
- 86. Pterygoids not visible in lateral aspect below ventral margin of jugal and quadratojugal = 0, or visible = 1
- 87. Pterygoid junction with squamosal along cheek margin: unsutured = 0, half and half = 1, sutured entirely = 2
- 88. Vomers separated by parasphenoid > half length: present = 0, absent = 1
- 89. Vomers separated by pterygoids: for > half length = 0, < half length = 1, not separated = 2
- 90. Vomer contributes to interptyergoid vacuity: absent = 0, present = 1
- 91. Vomers as broad as long or broader = 0, about twice as long as broad or longer = 1

#### Upper Dentition

- 92. Ectopterygoid fang pairs: present = 0, absent = 1
- 93. Ectopterygoid row (3+) of smaller teeth: present = 0, absent = 1
- 94. Ectopterygoid denticle row lateral to tooth row: present = 0, absent = 1
- 95. Ectopterygoid / palatine shagreen field: absent = 0, present = 1
- 96. Maxilla tooth number: > 40 = 0, 30-40 = 1, < 30 = 2
- 97. Maxillary caniniform teeth (about twice the size of neighbouring teeth): absent = 0, present = 1
- 98. Palatine fang pairs: present = 0, absent = 1
- 99. Palatine row of smaller teeth: present = 0, absent = 1

100. Palatine denticle row lateral to tooth row: present = 0, absent = 1
101. Parasphenoid shagreen field: present = 0, absent = 1
102. Parasphenoid shagreen field anterior and posterior to basal articulation = 0, posterior to basal articulation only = 1, anterior to basal articulation only = 2
103. Pterygoid shagreen: dense = 0, a few discontinuous patches or absent = 1
104. Premaxillary teeth with conspicuous peak: absent = 0, present = 1
105. Premaxillary tooth number: > 15 = 0, 10 - 14 = 1, < 10 = 2
106. Vomer fang pairs: present = 0, absent = 1
107. Vomerine fang pairs noticeably smaller than other palatal fang pairs: absent = 0, present = 1
108. Vomer anterior wall forming posterior margin of palatal fossa bears tooth row meeting in midline: present = 0, absent = 1
109. Vomerine row of small teeth : present = 0, absent = 1
110. Vomerine shagreen field: absent = 0, present = 1
111. Vomerine denticle row lateral to tooth row: present = 0, absent = 1
112. Vomer with toothed anterolateral crest: present = 0, absent = 1
113. Upper marginal teeth number: greater than lower = 0, same = 1, smaller than lower = 2

#### Lower jaw characters

114. Adductor fossa faces dorsally = 0, mesially = 1
115. Angular – prearticular contact: prearticular contacts angular edge to edge = 0, absent = 1, mesial lamina of angular sutures with prearticular = 2
116. Angular reaches posteriormost point of lower jaw: absent = 0, present = 1
117. Coronoid (anterior) contacts splenial: absent = 0, present = 1
118. Coronoid (anterior) contacts postsplenial: absent = 0, present = 1
119. Coronoid (middle) contacts postsplenial: absent = 0, present = 1
120. Coronoid (middle) separated from splenial: present, by prearticular = 0, absent = 1, present, by postsplenial = 2
121. Coronoid (posterior) posterodorsal process: absent = 0, present = 1
122. Coronoid (posterior) posterodorsal process visible in lateral view: absent = 0, present = 1
123. Coronoid: at least one has fang pair recognisable because at least twice the height of coronoid teeth: present = 0, absent = 1
124. Coronoid: at least one has fangs recognisable because noticeably mesial to vertical lamina of bone and to all other teeth: present = 0, absent = 1
125. Coronoid: at least one has organised tooth row: present = 0, absent = 1
126. Coronoid: at least one carries shagreen: absent = 0, present = 1
127. Coronoid with a row of very small teeth or denticles lateral to tooth row: present = 0, absent = 1
128. Coronoid: size of teeth (excluding fangs) on anterior and middle coronoids relative to dentary tooth size: about the same = 0, half height or less = 1
129. Dentary with parasymphysial fangs internal to marginal tooth row: present = 0, absent = 1
130. Dentary tooth number: more than 70 = 0, 56-70 = 1, 46-55 = 2, 36-45 = 3, less than 35 = 4
131. Dentary with a row of very small teeth or denticles lateral to tooth row: present = 0, absent = 1
132. Dentary external to angular + surangular, with chamfered ventral edge and absent interdigitations: absent = 0, present = 1

133. Dentary ventral edge: smooth continuous line = 0, abruptly tapering or 'stepped' margin = 1
134. Mandibular sensory canal: present = 0, absent = 1
135. Mandibular canal exposure: entirely enclosed, opens through lines of pores = 0, mostly enclosed, short sections of open grooves = 1, mostly open grooves, short sections opening through pores = 2, entirely open = 3
136. Mandibular oral sulcus/ surangular pit line: present = 0, absent = 1
137. Meckelian bone visible between prearticular and infradentary series: present = 0, absent = 1
138. Meckelian bone or space exposure in middle part of jaw, depth much less than prearticular = 0, depth similar to prearticular = 1
139. Meckelian foramina/ fenestrae, dorsal margins formed by; Meckelian bone = 0, prearticular = 1, infradentary (postsplenial) = 2
140. Adsymphyseal tooth plate: present = 0, absent = 1
141. Adsymphyseal plate fang-pair (distinct from other teeth): absent = 0, present = 1
142. Adsymphyseal plate dentition: shagreen, denticles or irregular tooth field = 0, organised dentition aligned parallel to jaw margin = 1, no dentition = 2
143. Adsymphyseal lateral foramen present: absent = 0, present = 1
144. Adsymphyseal mesial foramen present: absent = 0, present = 1
145. Postsplenial with mesial lamina: absent = 0, present = 1
146. Postsplenial pit line present: present = 0, absent = 1
147. Postsplenial suture with prearticular: absent = 0, present but interrupted by Meckelian foramina or fenestrae = 1, uninterrupted suture = 2
148. Prearticular shagreen field, distribution: gradually decreasing from dorsal to ventral = 0, well defined dorsal longitudinal band = 1, scattered patches or absent = 2
149. Prearticular sutures with surangular: absent = 0, present = 1
150. Prearticular with longitudinal ridge below coronoids: absent = 0, present = 1
151. Prearticular centre of radiation of striations: level with posterior end of posterior coronoid = 0, level with middle of adductor fossa = 1, level with posterior end of adductor fossa = 2
152. Splenial, rearmost extension of mesial lamina: closer to anterior end of jaw than to adductor fossa = 0, equidistant = 1, closer to anterior margin of adductor fossa than to the anterior end of the jaw = 2
153. Surangular crest: absent = 0, present = 1

#### General skull characters

154. Skull longer than broad = 0, as broad as long = 1, or broader than long = 2
155. Preorbital region of skull less than twice as wide as long = 0, or at least twice as wide as long = 1
156. Anterior palatal fenestra: single = 0, double = 1, absent = 2
157. Internarial/ interpremaxillary fenestra (independent of presence of median rostrals): absent = 0, present = 1
158. Interorbital distance compared with maximum orbit diameter: greater = 0, smaller = 1, subequal = 2
159. Interpterygoid vacuities: absent = 0, at least 2 x longer than wide = 1, < 2 x longer than wide = 2
160. Naris position: ventral rim closer to jaw margin than height of naris = 0, distance to jaw margin similar to or greater than height of naris = 1
161. Naris shape: slit-like = 0, round or oval = 1, upper margin ragged = 2

162. Naris shape: ventrally facing = 0, dorsolaterally facing = 1
163. Orbit shape: round or oval = 0, angle at anteroventral corner = 1, angle at posteroventral corner = 2: emarginated margin including jugal, lacrimal and prefrontal = 3
164. Orbit position re snout/postparietal length: centre closer to front than rear = 0, centre near middle = 1, centre closer to rear than front = 2
165. Orbit position re snout/quadrato length: centre closer to front than rear = 0, centre near middle = 1, centre closer to rear than front = 2
166. Pineal foramen position along interparietal suture: behind midpoint = 0, at the midpoint = 1, anterior to midpoint = 2
167. Suspensorium proportions: quadrato to anterior margin of temporal embayment about equal to maximum orbit width (discounting any anterior extensions) = 0, quadrato to anterior margin of temporal embayment < maximum orbit width = 1, quadrato to anterior margin of temporal embayment > maximum orbit width = 2
168. Skull table/cheek junction: smooth profile = 0, square/ abrupt profile = 1
169. Skull table shape: longer than broad = 0, approximately square = 1, shorter than broad = 2
170. Ornament character: regular, dense, but no star-burst pattern = 0, fairly regular pit and ridge with star-burst pattern at regions of growth = 1, irregular but deep = 2, irregular but shallow = 3, absent or almost absent = 4

#### Postcranial characters

171. Centra: intercentrum dominant = 0, pleurocentrum dominant = 1, holospondylous = 2
172. Centra strongly notochordal such that notochordal space more than 2/3 diameter of entire centrum: present = 0, absent = 1
173. Centra (trunk) pleurocentra fused midventrally: absent = 0, present = 1
174. Centra (trunk) pleurocentra fused middorsally: absent = 0, present = 1
175. Centrum (sacral) not distinguishable by size or shape from pre- and postsacrals = 0, distinguishable = 1
176. Clavicles meet anteriorly: present = 0, absent = 1
177. Cleithrum co-ossified with scapulocoracoid = 0, separate = 1
178. Cleithrum smoothly broadening to spatulate dorsal end = 0, distal expansion marked from narrow stem by notch or process or decrease in thickness = 1, end simply tapering = 2
179. Cleithrum stem cross section at mid section, flattened oval = 0, irregular = 1, single concave face = 2
180. Humerus ends more or less untorted = 0, ends offset by > 60 degrees = 1
181. Humerus L-shaped = 0, waisted but no shaft = 1, with distinct and slender shaft = 2
182. Humerus accessory foramina present = 0, absent = 1
183. Humerus latissimus dorsi process part of ridge = 0, distinct but low process = 1, spike = 2
184. Humerus latissimus dorsi process position compared with deltopectoral crest: more proximal to head = 0, equidistant from head = 1
185. Humerus latissimus dorsi process position relative to ectepicondyle: offset anteriorly = 0, in line = 1
186. Humerus latissimus dorsi process confluent with deltopectoral crest: present = 0, distinct from = 1

187. Humerus anterior margin: smooth finished bone convex margin = 0, anterior keel with finished margin = 1, cartilage-finished = 2, smooth concave margin = 3
188. Humerus radial facet position: distal and terminal = 0, anteroventral = 1, ventral = 2
189. Humerus radial/ulnar facets: confluent = 0, separated by perichondral strip of bone = 1
190. Humerus with distinct supinator process: absent = 0, present = 1
191. Humerus with ventral humeral ridge: present = 0, absent = 1
192. Humerus ectepicondyle distinct: present = 0, absent = 1
193. Humerus ectepicondylar ridge distal end aligned with ulnar condyle = 0, between radial and ulnar condyles = 1, aligned with radial condyle = 2
194. Humerus entepicondyle width relative to half humeral length: greater = 0, less = 1
195. Humerus entepicondyle width relative to humeral head width: smaller = 0, greater = 1
196. Interclavicle body shape (distinguished from parasternal process): rhomboid, longer than broad = 0, broader than long = 1
197. Interclavicle parasternal process shape: absent or tapering = 0, parallel sided = 1
198. Neural arch ossification: paired in adult = 0, single in adult = 1
199. Neural arch (atlas) halves fused: absent = 0, present = 1
200. Neural arches with distinct convex lateral surfaces ('swollen'): absent = 0, present = 1
201. Neural arches of trunk vertebrae fused to centra: absent = 0, present = 1
202. Radius: longer than ulna = 0, same length as ulna = 1, shorter than ulna (including olecranon process if present) = 2
203. Ribs (trunk): straight = 0, ventrally curved = 1
204. Ribs (trunk) not longer than height of neural arch plus centrum = 0, less than 2.5 x height of neural arch plus centrum = 1, more than 2.5 x height of neural arch plus centrum = 2
205. Ribs (trunk) tapered distally or parallel-sided = 0, expanded distally into overlapping posterior flanges = 1
206. Ribs (trunk) bear proximodorsal (uncinate) processes: absent = 0, present = 1
207. Ribs (trunk) differ strongly in length and morphology along 'thoracic' region: absent = 0, present = 1
208. Ribs (cervical): flared distally = 0, tapered distally = 1
209. Scapulocoracoid dorsal blade: absent = 0, small with narrow top = 1, large with broad top = 2
210. Scapular ossification separate from coracoid: absent = 0, present = 1
211. Gastralria: tapered and elongate, 4 or >4 x longer than broad = 0, ovoid = 1, around 3 x longer than broad one end tapering = 2
212. Pelvis: ilium, ischium, pubis not separate ossifications=0, separate=1
213. Ilium: post illiac process and dorsal blade present = 0, only post iliac process present = 1
- \*214. Dentary notch: absent = 0; present = 1
- \*215. Dentary chin: absent = 0; present = 1
- \*216. Neural and haemal spines flattened, rectangular or fan-shaped in lateral view absent = 0, present = 1
- \*217. Odontoid process: absent = 0; present = 1

- \*218. Accessory apophyses in at least some trunk and tail vertebrae: absent = 0; present = 1
- \*219. Transverse process length 30% or more than neural arch height: absent = 0; present = 1
- \*220. Postorbital ventrolateral digitiform process fitting into jugal: absent = 0; present = 1
- \*221. Supratemporal narrow, strap-like, at least three times longer than wide: absent = 0; present = 1
- \*222. Jaw articulation position: posterior to = 0, level with = 1, anterior to occiput = 2.
- \*223. Postorbital contribution to orbit: present = 0; absent = 1
- \*224. Parietals more (0) or less (1) than two and a half times as long as wide
- \*225. Postorbital not wider (0) or wider (1) than orbit
- \*226. Number of manus digits: absent (0); present 8 (1); present 6 (2); present 5 (3); present 4 (4).
- \*227. Number of pes digits: absent (0); present 8 (1); present 7 (2); present 6 (3); present 5 (4), present 4 (5).
- \*228. Extra articulations on haemal spines: absent = 0; present = 1.
- \*229. Postorbital extending lateral to orbit: absent = 0 present = 1
- \*230. Tabular ventral facets for braincase: none or indistinct = 0, single = 1, double = 2
- \*231. Parietal-parietal width smaller = 0 or greater = 1 than distance between orbits' posterior margin and skull table posterior margin, measured along midline of skull.
- \*232. L-shaped proximal tarsal element: absent = 0; present = 1.
- \*233. Postorbital anteromesial digitiform process fitting into posterior lappet of postfrontal: absent = 0; present = 1
- \*234. Supraorbital line on premaxilla runs parallel to jaw margin = 0; supraorbital line on premaxilla directed towards the jaw margin = 1; no supraorbital line present on premaxilla = 2
- \*235. Marginal teeth without = 0 or with = 1 a 'dimple'.
- \*236. Spinal nerve foramina: absent = 0, present = 1.
- \*237. Costal process of rib: absent = 0, present = 1.
- \*238. Temporal fenestra: absent = 0, present = 1.
- \*239. Maxilla not contributing = 0 or contributing = 1 to orbit margin.
- \*240. Olecranon process: absent = 0; present = 1.
- \*241. Cleithrum: ornamented = 0, not ornamented = 1
- \*242. Cleithrum, postbranchial lamina: present = 0, absent = 1
- \*243. Jugal: does not extend posterior to postorbital = 0, posterior process extending well beyond level of postorbital = 1
- \*244. Frontal: absent = 0, present = 1
- \*245. Opercular present = 0, absent = 1
- \*246. Splenial has free ventral flange: yes = 0, no = 1
- \*247. Basipterygoid process: not strongly projecting with concave anterior face = 0, strongly projecting with flat anterior face = 1
- \*248. Meckelian bone floors precoronoid fossa: yes = 0, no = 1
- \*249. Parasphenoid: does not overlap basioccipital = 0, overlaps basioccipital = 1

- \*250. Dentary teeth: same size as maxillary teeth = 0, larger than maxillary teeth = 1, smaller than maxillary teeth = 2
- \*251. Adsymphysial plate has tooth row: no = 0, short tooth row, separated from coronoid tooth row by diastema = 1, long tooth row reaching coronoid = 2
- \*252. Humerus: narrow tapering entepicondyle = 0, square or parallelogram-shaped entepicondyle = 1
- \*253. Pectoral process of humerus: absent = 0, present = 1.
- \*254. Proximal limb of oblique ridge of humerus: present, separated from anterior margin of humerus by prepectoral space = 0, absent, replaced by deltopectoral crest = 1
- \*255. Chorda tympani foramen not discernible (0), present and straddling articular-prearticular suture (1), present on prearticular only (2), or present on articular only (3).
- \*256. Postparietals paired (0), fused (1), absent (2).
- \*257. Interclavicle: small and concealed or absent = 0, large and exposed = 1
- \*258. Depth of postsplenial at level of postsplenial-dentary-angular triple joint about half of ramus depth at the same level (0), more than half (1), less than half (2).
- \*259. Constriction between dorsal and ventral margins in the posterior part of prearticular mesial surface absent (0) or present (1).
- \*260. Ethmoid: fully ossified = 0, partly or wholly unossified = 1

**Data matrix as nexus format with multiple character-states in round and curly brackets denoting, respectively, polymorphism and uncertainty**

#NEXUS

BEGIN TAXA;

DIMENSIONS NTAX = 57;

TAXLABELS

*Acanthostega Asaphstera Balanerpeton Baphetes Diploradus Ossirarus  
Caerorhachis Casineria Colosteus Crassigyrinus Dendrerpeton Doragnathus Discosauriscus  
Edops Eoherpeton Eryops Eucritta Eusthenopteron Gephyrostegus Greererpeton Hyloplesion  
Ichthyostega Loxomma Metaxygnathus Megalocephalus Microbrachis Occidens Ossinodus  
Paleothyris Panderichthys Pederpes Pholiderpeton Proterogyrinus Seymouria Sigournea  
Silvanerpeton Tiktaalik Tulerpeton Ventastega Westlothiana Whatcheeria Koilops Ymeria  
Perittodus Aytonerpeton Acherontiscus Adelogyrinus Adelospondylus Dolichopareias  
Ptyonius Sauroplesura Urocordylus Lethiscus Oestocephalus StLouisTetrapod Elginerpeton  
Densignathus*

;

END;

BEGIN CHARACTERS;

DIMENSIONS NCHAR = 260;

FORMAT DATATYPE = STANDARD GAP = - MISSING = ? SYMBOLS = "0 1 2  
3 4 5";

MATRIX

*Acanthostega*

0000000001001???0000001000010011000000110100000010000000100000  
0100010001010000?1211000011?0100000000020010000000101010000?11

*Asaphestera*

## Balanerpeton

*Baphetes*

*Diploradus*

*Ossirarus*

*Caerorhachis**Casineria*

*Colosteus*

```
1????0???1111???11?00?02010101020110?0121100100111???1110110000
110000001?1112???1?21100?1100001010011?0011?100110120???0???
0?1?041010{12}?111????0???1????001?0101100002001?000?01?????
???????????001?001???1????0?100?010001014?00?0?0100000????11
11?11?????012??
```



```

1??1?00??200000000?0000101110012100??0021111000001000100211211
0001111?000111110122?00011000001010001020000001010102?00000?11
111?141010311010010001010012000111012111002102?01??11?10011111
200010?11000000112000???010?00?00000010??0020?0?000000111111?1
1(01)01110011??

```

```

1????1???00000101100100101110002100??0021100101002??0001?12220
1001001???111200?012011021211????0001101001011111101201??11?11
11???31011?1101?????11{12}210?{01}1002101111011101210000?111?1
12????32?010?1?00??00211000010111?00?000000104?01?000200000111
?111111(01)?111101211

```

```

????????????????????????????????????????????????????????????????????????????????
????????????????????????????????????????????????????????????????????????????020?????0?11
0011101011?11011??001112?0?{12}01????????????????????????????????????002{
01}???{01}00010{12}1000????????????????11?0????????????????????????????0?
?????????????1????11??121?

```

```
0111?001020101111101010100011002100??1021111101002100000012221
1001100201112?0111?011111001111020011020020011011212110001111
1111131010311?11??00112200?221120210110012112311111012?0021001
300010?1?111110211001011110?00000001010340111?000000?011?111?1
10?11120121?
```

```
0111111101000010000010001011000200011002010010111211000?11?2?1
100?101101111200?102111?212000111200110?0020111111212?1???1?11
111?0310?1?1??????0011??10???002001101022020210?00?????112????
32?111?11??????????1?1???00?00000011???1?0?0?0??00?11?11111
10?111101??1
```

```

????????100000011?010011?0100?2100??10211?100?0021?0000?1121?
0000100?0?01??111?221?1?????101020011?0002?????????1????11
0111???0?1?1101?????1112?022200?10?011011211221110???1???0020011
010110201??1?00?1200??1??10?0000000?010??0?10?0200000???1111?1
10?111?0???1

```

```
0?11111111001??0001100010110002100110010100101002110011112211
1000010101112300??020110212100111110111?0110111111112111021111
111?021011?11?1???00112210?01002001111022021210100111121121101
320110201101000201011010?11?00000(01)000104401?000200000111?11
11110?111201211
```

```
1????????200001010?000010?010002?00??002111010{01}002??000??11
2201001000????1?110?1121?1?????????110??000??0????????????
?????????0?1?1????????????????000?01?????12111?21?????110?02?
????????????00?0??0?00?01?010?0???000010?4?000?0?0?000?11?11
1???0?111?01???
```

[illegible]

[illegible]

??100???01  
0011??1010???10?????010????????????????????????????????????2????????????????????  
??  
??????????2??

*Ossinodus*

????10?????1????010000?0?0100????0??01211011?00120???0??01211  
1001000?0111?????????1?00?1100101001001???0?1000000????????????  
??????????020?????????000??????001?200?1?100011?????????????1????  
?????????????????????????1?000????????????0?????????0?0??1111?1?  
???111?01???

*Paleothyris*

1?11100001011????10?1010100011002100?011211121010021000100112?0  
?0010002???1?120?1?2111101201???011111021021?11111???1????????  
?????????11?1?????????1??????1002011011011211131111101??122????  
32011021?1110012120001102??0000000010103400?110200000111?1111?  
10?111?01???

*Panderichthys*

00000000000?000000?00000000200000??100000100100110000000001210  
010000000?00??0000?000??002000000??000?2?0?00000?0?00?00?00?00  
00000?00000000000000000000?00000000000?00121000000??10?000000?  
000000010??0?00000000?00?10000?000000010001?0?0000000000010000  
000000000000

*Pederpes*

1????0?????01?111??0??10?00000?1????00??100?100021?0010?01230  
10011002010?03?101?210???11?00011210010?0?20010111??{01}1?????  
???0??1?????0?1??????????0?????000??0021221?21210000011110022  
1012??110?0?000000102111011210000?000000?0{234}{234}?0?1?0?000  
00011111?1?1?111??1???

*Pholiderpeton*

0?111001010001100110100210010002100201020110100002100000110?11  
000111120001111111021010011010010010111?0021?110111121100?1111  
111??31010201110020011211?220020210210221011211111111?0?????  
????1011?0010002120000102??000?00000010?012??0200000111?11111  
1??111201{01}01

*Proterogyrinus*

1?111001010001001100?011??0100020000010211100010021000?0?11211  
000121120001131111021111?????110100001101002?????????11201000??0?  
?1??021011?1111??0??1?211?2200?0210110212211311101111?0021111  
22?11000100100021200001021000000000001034002010200000111111111  
10?111?0110?

*Seymouria*

0?111011020001110101010100111002100211021101101002110000012221  
10010002011111111221011210011111200111?0020011011212110001111  
111??41001?11?11??00112200?220020000111112012111111011111211?1  
321111?10111111211101011?100000000010103401?1?0200000111111111  
1??111?012?1

*Sigournea*

??  
??2?10001?11  
0011001010310010??000102?0?{01}{01}????????????????3?????????  
????????????????????????????????????00????????????????????0?????  
???0?1??0???0??2??

*Silvanerpeton*

1?1110???200010011?001010??11002100??102?111001001??0010?11011  
0100200???11?110?122101??1001???11001100002??????11?1??????11  
111??21011????1?????1?12?0??{12}002010011011211031010?111?002?  
???1????0?1000?000212000010210000?0000001?3400?000200000011011  
?1?10?111?01???

*Tiktaalik*

?????0?????1???00?11???0????????????000110000110??1?0??01211  
0001000????????0?020000??0?0????????????????????00000000?00  
00?0??10000?0000??000??000??000?0200?012102020??????10?000????  
001000110??????00?100?00?0?000?000000?100?1?0?0?0?00000011?00  
0?0000?00100

*Tulerpeton*

????????????????1?1?101????????????????02?100????????????01?????  
?001010????????????????????0????????????110?10111??2?????????  
????????02????????????????????????????2???100???01111021011  
00111010100????21?????1001000????????23????1??0????11???????  
???111??1???

*Ventastega*

00????????000?1000101001100100?11?000?11010010000?000010?012?0  
?0??0010??1102????0?1000?1?000?000001100110000010200010000?01  
001100110010001001110001010000001200??121?2101????0000??????  
?????????00????????????0????00????0?00?0???0?0?0?0?0?0?11111001  
002???1?1101

*Westlothiana*

?????0???1011???10??0???0?01?0?2100??112111010100??????0?102?1  
0000000????1??10?1?21000?1?0????120???1?001???????1??1????????  
?????210?1?1????????????????{12}00?000011011111241111??1??122?  
???32?11121???1?01212000110?11000?00001010{34}400?11020000?1??  
?1111?1???111?01???

*Whatcheeria*

?????00??110001111?110011?0100?2100100010100100001100000?01211  
10011012????????10??21????????001011001??0120??000?111010001011  
0011031000{12}100001100010101120???01002122200?2400101011?022  
10120?0?0101111?002??11??11?10000?00000010??0011?0000000110111  
0?112111110120?

*Koilops*

????????????010????10?10??1?????1?2??????02?1101?000???0000?????1  
????????0??????1????????????0??????0?????20?0?????????????  
????????????????????????????????0122??11011????1?????????????  
????????????????????????????????0?{01}0?0???1???0???0?????1?  
????????????????

*Ymeria*

????????????????????????????1?????????????????????????????  
????????00?0????????100????0?001?21001???0200100111000?0000?01  
001004110021001011?1010100000?????????????????????????????  
????????????????????????????00????????????????????0??????????0?  
?01??????1??

*Perittodus*

????????????????11?{01}??0???01??0?????????????????????????  
????????????????????????????????20????????????????????010?10  
?01001014100??????011??0????1?0????????????????3???????????

????????????????1??????0??00????????????????0?????????  
????????0??10?

*Aytonerpeton*

????????????????00?10001000?1?????????????????????  
????????????????0????????200?1??0120111?1?0???1001??11  
10101410?010??100????0???{12}01????011????2?????????  
????????????0?0?????1100????????????0??0?????  
?????????????

*Acherontiscus*

????????2111???10?001010?0100??111???121000?0011???1100?12??0  
??1??????1?1????22??0????????20????002??????0??1??????  
?1???4101010????????????201?001?110000100?1?11?????????  
????????0??????{01}{01}00?????0?0?010?1101??00?0?0?00000??  
?11????0??????12??

*Adelogyrinus*

??11????00111???10?00002???101?211????121100?00001??0?0??12??{  
01}??1????????????????????{01}????????????????1??  
??????????{23}?0102????????1??????{12}01??0????00001001????  
??10????????????00????????????01?0?10?1100???0?0?0?1?  
?01????11????0?????012??

*Adelospondylus*

????????2111???1000010{01}0???00????????21101?????01?100??12  
??1??1????11??11??????000?????1111???11?0??????????1?????  
????????{23}10102??????????????{12}0{12}??{02}1???000110012  
111????????????????1?00?0{01}010???0?010?01??1?0?????  
0???1000?????1????0?????012??

*Dolichopareias*

????????0111???10?00?0?0?1{01}0??2111???121101?00111??1100??{  
12}?????1????????????????????{01}0?????02?????????  
????????????????????????????????01?00?11?00001001??????  
????????????????????????????????0??101???0?0?0?1?0?  
????1??????????0????

*Ptyonius*

1????0???1101???110001010?010002100??1121100000010??0100?11201  
0001000?0?011200?1221100???001?0201011?1021?10011{12}1?1????0  
?11101?141011?1???1?????1?????20020110110002101121110110?002?  
???32?0???100011011110001100110011101110014511?0?1200000111?11  
11?10?111?01???

*Sauropleura*

1????0???11{01}1???100000010?0{12}00021(01)0??1121{01}0{01}000  
{01}1(01)??1100?110010100000???011{12}{01}0??22?100????1???020  
1011?00{12}1?10011{12}1?1????0?11101?1{24}1011?11?11????1?2??  
?220020110110{02}{02}210012111011{01}?002???32?1???1000110111  
10001100110010101100014411?00120000111?1111110?111?01?0?

*Urocordylus*

????0????????11000?0?0?010????????????0001?????0?11???  
01????????0????????1????????20101??002??????{12}??????0  
?11101?141011?1???1????????{12}00???10??000?1?0?21110111?0  
02????12?0???000011011110001100110010101??0?13411???1200000111  
?1111????111??1???

*Lethiscus*

????????{12}?1????10??00010??100?2?11???121100?00?1???0000{01

}?{01}?000?0?????110??{13}?0?0?0?0?0?0?0?0?0?010101?????????  
????????????????410????0010021101?2?1?2000?01???1100021???2011  
0????????????????1?01?0?0001??0?????0001000100?1?0?0??1  
111????111?1000????10??1

*Oestocephalus*

??0100???0011???100100010?0100021111???21101?????(01)1?1100?1{  
01}000010?0002???11?100??22?000???????0101011?102???????21?1??  
???????????121011?11??1???????210?200020110110000102?2?11?????  
????????????????1?01?1{01}0001??0??0001???10?0?????????201111  
????11111???????0????

*StLouisTetrapod*

0????????????????????0?0?0?0?0?0?0?0?0?0?0?0?0?0?0?0?0?0?0?  
?????????1????????????11?0111?0011?0?2????1?????????????  
????????0?021???0????????????{12}01???0?????????????????  
????????????????????10????????????????10?????????1?  
???????????????

*Elginerpeton*

???  
??1??????10  
00?0?0000000001111000101?1?????????????????????????????????  
??11?????1  
??1??????2??

*Densignathus*

???  
??01?1???0?00  
00?1???110000000011110?0100000?0?????????????????????????????  
??0?1  
??1??????{01}0?

;

END;